

RESEARCH ARTICLE

Cite this: *RSC Med. Chem.*, 2023, 14, 2327

Synthesis of 2-aminopropyl benzopyran derivatives as potential agents against triple-negative breast cancer†

Ainhoa García, ^{ab} Sandra Torres-Ruiz,^b Laura Vila, ^b Carlos Villarroel-Vicente,^{ab} Álvaro Bernabeu,^a Pilar Eroles,^{*bcd} Nuria Cabedo ^{*ab} and Diego Cortes ^a

Synthesis of three series of 2-aminopropyl derivatives containing a benzopyran nucleus was performed to evaluate their performance against triple-negative breast cancer cell lines (MDA-MB-231 and MDA-MB-436) and normal breast epithelial cells (MCF10A). For the three series, the cytotoxic activity was as follows: *N*-methylated derivatives (tertiary amines) **5b**, **6b**, and **7b** > secondary amine benzopyrans **5**, **6**, and **7** > quaternary amine salts **5c**, **6c**, and **7c** > free phenolic derivatives **5a**, **6a**, and **7a**. The structure–activity relationship showed the importance of the presence of an amine group and a *p*-fluorobenzyloxy substituent in the chromanol ring (IC₅₀ values from 1.5 μM to 58.4 μM). In addition, **5a**, **5b**, **6a**, and **7b** displayed slight selectivity towards tumor cells. Compounds **5**, **5a**, **5b**, **6**, **6a**, **6c**, **7**, and **7b** showed apoptotic/necrotic effects due to, at least in part, an increase in reactive oxygen species generation, whereas **5b**, **5c**, **6b**, **7a**, and **7c** caused cell cycle arrest in the G1 phase. Further cell-based mechanistic studies revealed that **5a**, **6a**, and **7b**, which were the most promising compounds, downregulated the expression of *Bcl-2*, while **5b** downregulated the expression of cyclins *CCND1* and *CCND2*. Therefore, 2-aminopropyl benzopyran derivatives emerge as new hits and potential leads for developing useful agents against breast cancer.

Received 2nd August 2023,
Accepted 5th September 2023

DOI: 10.1039/d3md00385j

rsc.li/medchem

1. Introduction

Breast cancer (BC) is a complex and heterogeneous disease, and the most frequently diagnosed and leading cause of cancer-related deaths in women, with increasing mortality rates affecting more than 1 million women worldwide.^{1–4} The selection of drug therapy for patients depends on the cancer subtype: hormone receptor-positive, human epidermal growth factor receptor 2 (HER-2), and triple-negative BC (TNBC).

TNBC is characterized as lacking estrogen receptors (ERs), progesterone receptors (PRs), and HER-2.^{5–9} This is the most aggressive subtype, and represents 15% of all breast cancers.¹⁰ Consequently, TNBC patients do not respond to hormonal and anti-HER2 monoclonal antibody trastuzumab-based targeted therapies. An affordable therapeutic strategy includes cytotoxic chemotherapy with taxane- and

tetracycline-based combination treatment and platinum-based agents, but drug resistance is one of the major challenges that is currently being addressed by TNBC research.^{10,11} The discovery of new compounds that decrease the survival of tumor cells in this particular subtype of breast cancer is highly significant for enhancing treatment of this disease.¹⁰

Several natural products containing a benzopyran skeleton (Fig. 1) have exhibited anti-tumor properties against BC through pleiotropic mechanisms involving apoptosis and cell cycle arrest, among others. Genistein, an estrogenic soy-derived compound belonging to the isoflavone class, induces apoptosis in TNBC cells.^{12–15} Wogonin, a natural flavone isolated from the roots of *Scutellaria baicalensis* Georgi, suppresses tumor angiogenesis

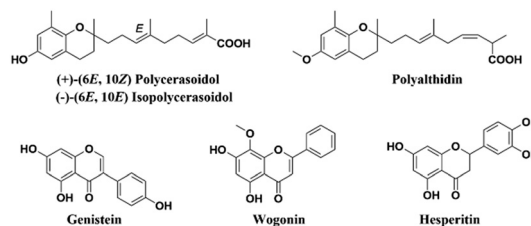


Fig. 1 Natural products containing a benzopyran skeleton.

^a Department of Pharmacology, University of Valencia, 46100 Valencia, Spain.
E-mail: ncabedo@uv.es

^b Institute of Health Research-INCLIVA, University Clinic Hospital of Valencia, 46010 Valencia, Spain

^c Department of Physiology, University of Valencia, 46010 Valencia, Spain.
E-mail: pilar.eroles@uv.es

^d Center for Biomedical Network Research on Cancer (CIBERONC), 28019 Madrid, Spain

† Electronic supplementary information (ESI) available. See DOI: <https://doi.org/10.1039/d3md00385j>



in BC.^{16,17} Moreover, hesperitin derivatives also present anti-tumor activity against BC.^{18,19} Therefore, the synthesis of the benzopyran nucleus has been performed by numerous medicinal chemistry groups in their search for new anti-tumor agents.^{20,21}

Our research group previously isolated polycerasoidol and polyalthidin (Fig. 1) from the stem bark of *Polyalthia cerasoides* (Annonaceae).^{22,23} Polycerasoidol and synthetic analogs displayed PPAR-activating properties, anti-inflammatory effects, and ameliorated metabolic derangements,^{24,25} while it has been shown that polyalthidin is an inhibitor of the mammalian mitochondrial respiratory chain.²³ In addition, it has been reported that isopolycerasoidol induces mitochondrial-mediated apoptosis in human BC cell lines.²⁶

Based on these pieces of evidence, our goal was to discover new molecules for future TNBC treatment. Therefore, we synthesised 2-aminopropyl benzopyran derivatives bearing a *p*-methoxyphenylethylamine (series 1), diphenylethylamine (series 2), or isoquinoline moiety (series 3) (Scheme 1). The 15 new compounds were tested against human TNBC cell lines (MDA-MB-231 and MDA-MB-436) and normal breast epithelial cells (MCF10A) for cytotoxic activity. Then, we studied their impact on the apoptosis/necrosis effect or cell cycle arrest, as well as their reactive oxygen species (ROS) production and the gene expression of some promising compounds.

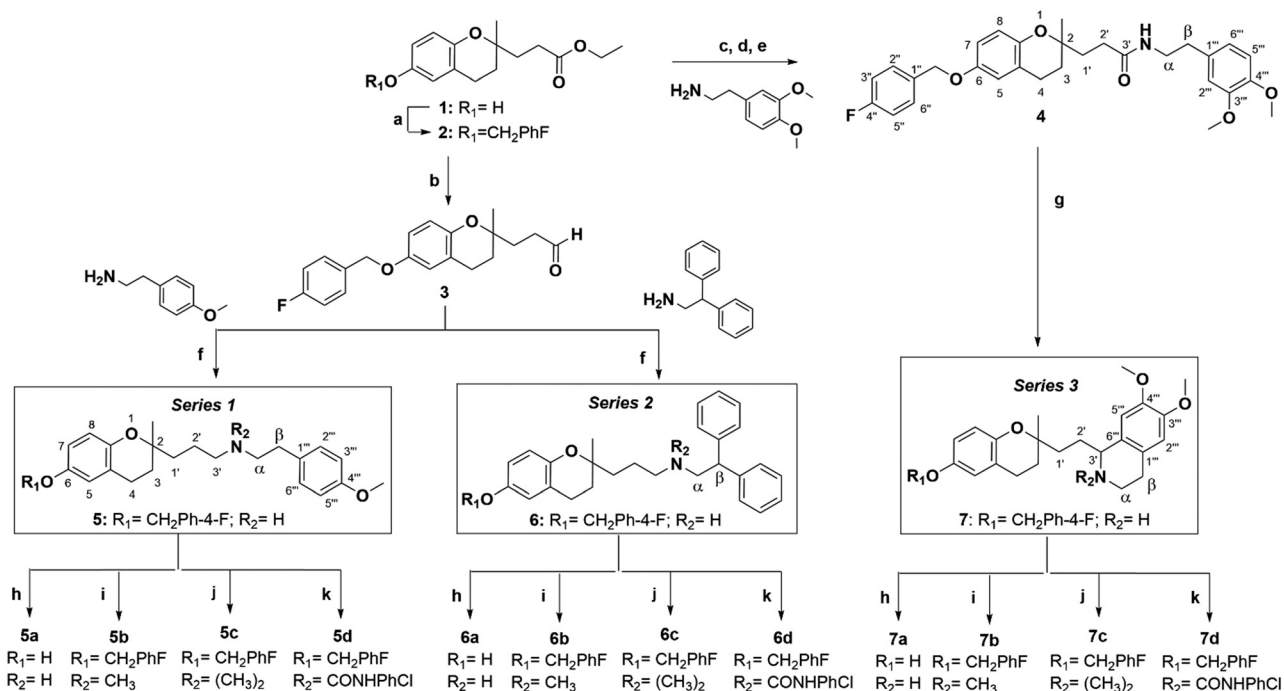
2. Results and discussion

2.1. Chemistry

Using different methodologies, we synthesized three series of compounds with a benzopyran skeleton. 2-Aminopropyl benzopyran derivatives were synthesised *via* a chroman-4-one scaffold. These derivatives were obtained by aldol condensation between *o*-hydroxyacetophenones and methylketones in the presence of a secondary amine by Michael addition, as previously reported.^{27–30} The free phenolic group of precursor benzopyran **1** was protected using *p*-fluorobenzyl chloride in the presence of potassium carbonate to afford benzopyran ester **2** (Scheme 1).

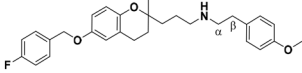
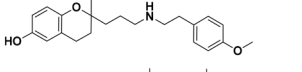
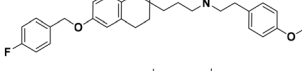
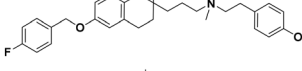
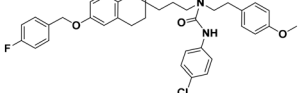
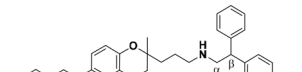
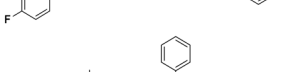
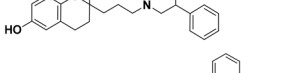
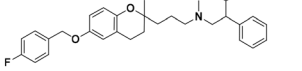
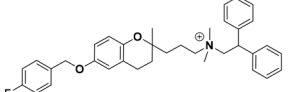
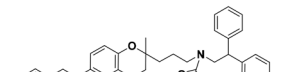
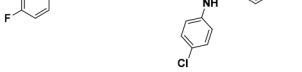
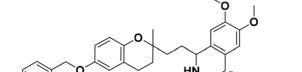
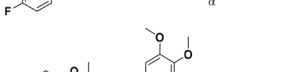
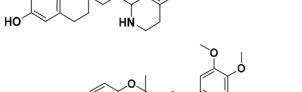
To obtain 2-aminopropyl benzopyran derivatives, two different synthetic pathways were followed from benzopyran ester **2**. The first was to synthesise *p*-methoxyphenylethylamine derivatives (series 1) and diphenylethylamine derivatives (series 2), and the second was used to synthesise isoquinoline derivatives (series 3). For the first pathway, controlled reduction by diisobutylaluminum hydride (DIBAL-H) of the ester group was carried out to obtain aldehyde intermediate **3**, from which compounds **5** (series 1) and **6** (series 2) were obtained by reductive amination.

The condensation of **3** with 4-methoxyphenethylamine and 2,2-diphenylethylamine resulted in secondary amines **5** and **6**, respectively, *via* a Schiff base, followed by reduction with sodium triacetoxyborohydride under acid conditions.



Scheme 1 Reagents and conditions: (a) *p*-fluorobenzyl chloride, K₂CO₃, EtOH, reflux, N₂, 4 h, 79%, (b) DIBAL-H, DCM, -78 °C, N₂, 15 min, 92%, (c) MeOH, KOH 20%, reflux, N₂, 4 h, (d) SOCl₂, DCM, reflux, N₂, 3 h, (e) 4-DMAP, Et₃N, DCM, rt., N₂, overnight, 63%, (f) NaBH(OAc)₃, AcOH, (CH₂Cl)₂, rt., N₂, 1 h, 72% for **5** and 54% for **6**, (g) POCl₃, CH₂Cl₂, reflux, N₂, overnight, NaBH₄, MeOH, rt., N₂, 2 h, 53%, (h) HCl:EtOH 1:1, reflux, N₂, 3 h, 92–96%, (i) HCHO, HCO₂H, MeOH, reflux, N₂, 1 h, NaBH₄, rt., N₂, 45 min, 76–86%, (j) MeI, DMF, reflux, N₂, 30 min–1 h, 79–96%, (k) 4-chlorophenyl isocyanate, Et₃N, DCM, rt., N₂, overnight, 68–92%.

Table 1 IC₅₀ values in TNBC and normal breast epithelial cells, and selectivity index (SI)

Structure	MDA-MB-231 (μM)	MDA-MB-436 (μM)	MCF10A (μM)	SI MCF10A/MDA-MB-231	SI MCF10A/MDA-MB-436
	13.2 ± 1.6 ^a	13.0 ± 2.0	6.3 ± 0.9	0.48	0.48
	51.0 ± 5.8 ^a	30.9 ± 3.5 ^a	76.8 ± 0.5 ^b	1.51	2.50
	7.3 ± 0.7	12.6 ± 1.5	12.1 ± 2.8	1.65	0.96
	25.0 ± 1.1 ^c	24.0 ± 1.2 ^b	25.0 ± 2.0 ^a	1.0	1.0
	>100	>100	>100	—	—
	11.0 ± 2.6 ^a	19.3 ± 0.8 ^b	12.9 ± 1.8 ^a	1.17	0.67
	48.3 ± 4.2 ^a	31.1 ± 5.5 ^c	46.6 ± 3.6 ^b	0.96	1.5
	1.5 ± 0.1	2.0 ± 1.7	1.4 ± 0.7	0.94	0.70
	19.2 ± 2.9 ^b	24.6 ± 1.1 ^b	20.8 ± 4.0	1.09	0.84
	>100	>100	>100	—	—
	22.2 ± 1.8 ^a	22.0 ± 0.8	21.9 ± 3.8	0.98	0.99
	58.4 ± 4.0 ^a	55.2 ± 5.6 ^a	54.2 ± 3.7 ^b	0.93	0.98
	14.0 ± 0.8	21.8 ± 0.6	20.1 ± 1.9	1.44	0.92
	42.2 ± 4.9 ^a	53.5 ± 1.1 ^c	41.4 ± 2.1 ^b	0.98	0.77
	>100	>100	>100	—	—
TMX	25.9 ± 0.1	15.80 ± 0.7	26.8 ± 0.5	1.03	1.70

The data are presented as the mean ± SD of three independent experiments performed in triplicate. ^a *P* < 0.05. ^b *P* < 0.01. ^c *P* < 0.001 vs. **5b**, **6b**, and **7b** for each family. Selectivity index (SI): ratio of cytotoxicity in MCF10A cells compared to that in cancer cells.

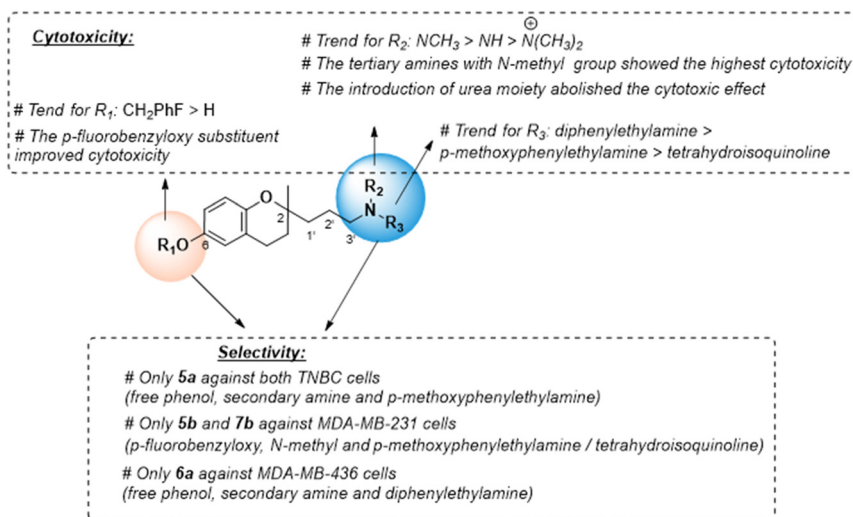


Fig. 2 SAR study of 2-aminopropyl benzopyran derivatives as potential anti-TNBC agents.

The second pathway was based on the formation of the amide intermediate **4** from an acid chloride. The ester group of **2** was submitted to basic hydrolysis, followed by a reaction with thionyl chloride. Then, acid chloride was reacted with 3,4-dimethoxyphenethylamine to yield amide **4**, from which compound **7** was obtained by Bischler–Napieralski cyclodehydration.

In each series, four derivatives were obtained from amines **5**, **6**, and **7**. The subsequent acid hydrolysis of the *p*-fluorobenzyl group yielded amines **5a**, **6a**, and **7a**. *N*-Methylated derivatives **5b**, **6b**, and **7b** were obtained with formic acid and formaldehyde, followed by reduction with sodium borohydride, while *N*-dimethylated salts **5c**, **6c**, and **7c** were obtained with methyl iodide. The functionalization of the amine group in the urea group was achieved by reacting it with 4-chlorophenyl isocyanate to obtain urea derivatives **5d**, **6d**, and **7d** (Scheme 1).

2.2. Pharmacology

2.2.1. Cytotoxicity evaluation and structure–activity relationships (SAR) study. The cytotoxicity of all the synthesised compounds against human breast MDA-MB-231 and MDA-MB-436 cell lines, and MCF10A cells was evaluated by the WST-1 assay. A dose–response curve analysis was performed to determine the drug concentrations required to inhibit cancer cell growth by 50% (IC_{50}) after 48 hours of incubation (Table 1).

For the three series, it was observed that the compounds were equally cytotoxic to cancer and normal cells. In the MDA-MB-231 cell line, the cytotoxic activity of the *N*-methylated compounds **5b**, **6b**, and **7b** (IC_{50} = 1.5–14.0 μM) was more potent than that of secondary amines **5**, **6**, and **7** (IC_{50} = 11.0–22.0 μM), followed by *N*-dimethylated derivatives as quaternary ammonium salts **5c**, **6c**, and **7c** (IC_{50} = 19.2–42.2 μM), as well as secondary amines with a free phenolic group **5a**, **6a**, and **7a** (IC_{50} = 58.4–48.3 μM).

In the MDA-MB-436 cells, the *N*-methylated compounds **5b**, **6b**, and **7b** (IC_{50} = 2.0–21.8 μM) were also more potent than secondary amines **5**, **6**, and **7** (IC_{50} = 13.0–22.0 μM), followed by *N*-dimethylated derivatives **5c**, **6c**, and **7c** (IC_{50} = 24.0–53.5 μM), and secondary amines with a free phenolic group **5a**, **6a**, and **7a** (IC_{50} = 30.9–55.2 μM).

In the MCF10A cells, *N*-methylated compounds were more potent than secondary amines, followed by *N*-dimethylated derivatives, and secondary amines with a free phenolic group. However, urea derivatives (**5d**, **6d**, and **7d**) did not produce any cellular cytotoxicity in either cell line.

For the three series, the structure–activity relationships (SAR) indicated that the nitrogen atom in the 2-propyl chain and the phenolic group in the benzopyran nucleus play a key role in cytotoxicity (Fig. 2). The tertiary or secondary amine function led to the most potent cytotoxic compounds, especially those bearing the *N*-(2,2-diphenylethyl) moiety (series 2), while its quaternization giving a ‘permanent cation’ decreased the cytotoxicity, which was most likely due to the difficulty in diffusing across cell membranes.

Urea-based derivatives are of growing interest for drug design and development, including anticancer drugs.³¹ However, the introduction in the 2-aminopropyl benzopyran of the *p*-chlorophenyl urea moiety increased the steric hindrance, which was detrimental for cytotoxic activity. The presence of the lipophilic *p*-fluorobenzoyloxy substituent in the chromanol ring favored cytotoxic activity, and its removal to a free phenolic group diminished the antitumor effect.

We also examined the selectivity of each compound against non-tumorigenic MCF10A cells. The selectivity index (SI) was calculated as the IC_{50} ratio of normal cells to cancer cells, $\text{SI} = \text{IC}_{50}(\text{MCF-10A})/\text{IC}_{50}(\text{MDA-MB-231 or MDA-MB-436})$ (Table 1). Four compounds showed slight selectivity against malignant cells. Of those, compound **5a** (secondary amine and free phenolic group) bearing the *p*-methoxyethylamine moiety (series 1) suppressed the growth

of both cancer cell lines with higher SI, and **5b** (tertiary amine and *p*-fluorobenzyloxy) displayed selectivity against MDA-MB-231 cells. Similarly, compound **6a** (secondary amine and free phenolic group) bearing the diphenylethylamine moiety (series 2) and compound **7b** (tertiary amine and *p*-fluorobenzyloxy) with the isoquinoline moiety (series 3) were selective against MDA-MB-436 or MDA-MB-231 cells, respectively. However, the most cytotoxic compound, **6b**, did not exhibit selectivity against cancer cells (Fig. 2).

Compounds **5a**, **5b**, **6a**, and **7b** with higher SI values were selected to carry out further mechanistic studies.

2.2.2. Studies of apoptosis and necrosis. To determine the cause of cell death, we evaluated the apoptotic and necrotic effects of cytotoxic compounds. For this purpose, TNBC cells were treated with each compound at concentrations equal to their respective IC₅₀ values (Table 1), followed by Annexin V-FITC and propidium iodide (PI) staining. Representative flow cytometry dot plots showing the effects in MDA-MB-231

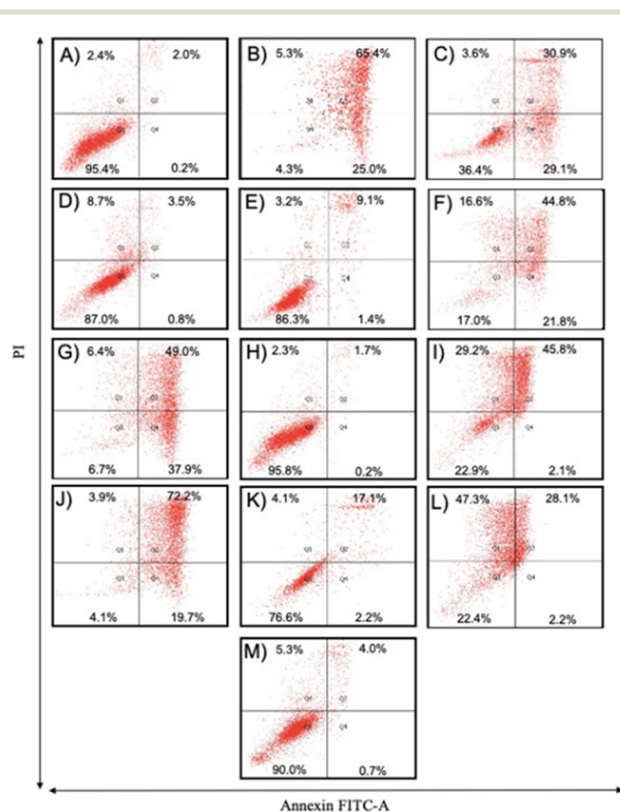


Fig. 3 Apoptosis/necrosis analyses of TNBC cells treated with compounds at their respective IC₅₀ values of cytotoxicity after Annexin V-FITC/PI staining. (A–M) Representative flow cytometry dot plots showing the effects of vehicle or compounds on MDA-MB-231 cell apoptosis/necrosis/survival have been included: (A) 0.1% DMSO, (B) **5** at 13.2 μM, (C) **5a** at 51.0 μM, (D) **5b** at 7.3 μM, (E) **5c** at 25.0 μM, (F) **6** at 11.0 μM, (G) **6a** at 48.3 μM, (H) **6b** at 1.5 μM, (I) **6c** at 19.2 μM, (J) **7** at 22.2 μM, (K) **7a** at 58.4 μM, (L) **7b** at 14.0 μM, (M) **7c** at 42.2 μM. (N) Histograms show the percentage of apoptotic and necrotic cell distribution. The data are expressed as the mean ± SD of three independent experiments performed in triplicate. ***P* < 0.01, ****P* < 0.001, *****P* < 0.0001 vs. DMSO group.

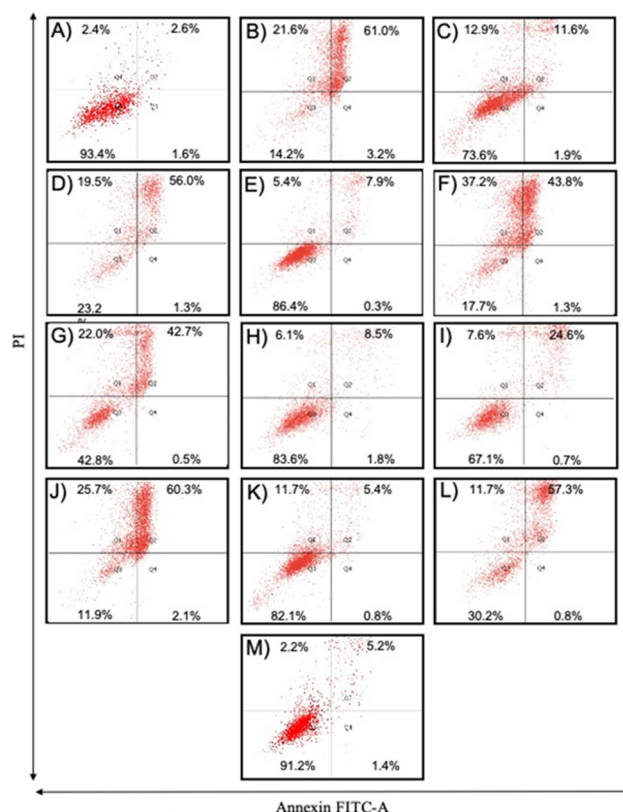


Fig. 4 Apoptosis/necrosis analyses of TNBC cells treated with compounds at their respective IC₅₀ values of cytotoxicity after Annexin V-FITC/PI staining. (A–M) Representative flow cytometry dot plots showing the effects of vehicle or compounds on MDA-MB-436 cell apoptosis/necrosis/survival have been included: (A) 0.1% DMSO, (B) **5** at 13.0 μM, (C) **5a** at 30.9 μM, (D) **5b** at 12.6 μM, (E) **5c** at 24.0 μM, (F) **6** at 19.3 μM, (G) **6a** at 31.1 μM, (H) **6b** at 2.0 μM, (I) **6c** at 24.6 μM, (J) **7** at 22.0 μM, (K) **7a** at 55.2 μM, (L) **7b** at 21.8 μM, and (M) **7c** at 53.5 μM. (N) Histograms show the percentage of apoptotic/necrotic cell distribution. The data are expressed as the mean ± SD of three independent experiments performed in triplicate. **P* < 0.05, ***P* < 0.01, ****P* < 0.001 vs. DMSO group.

and MDA-MB-436 cells are included in Fig. 3A–M and 4A–M, and histograms show the percentage of apoptotic and necrotic cell distribution in Fig. 3N and 4N, respectively. We observed that most cytotoxic compounds triggered apoptosis and necrosis. For both cancer cell lines, secondary amines **5**, **6**, and **7** significantly induced cell apoptosis and necrosis (83–96.5%), as did **6a** and **7b** (65–93%).

Compounds **5a** and **6c** induced a significant percentage of apoptotic and necrotic cells in the MDA-MB-231 line (64% and 75%, respectively), and to a lesser extent in the MDA-MB-436 line (30% and 32%, respectively). Significant apoptosis and necrosis were elicited by compound **5b**, but only in the MDA-MB-436 cell line (74%). In addition, ROS are crucial in inducing apoptosis through several pathways. Therefore, the

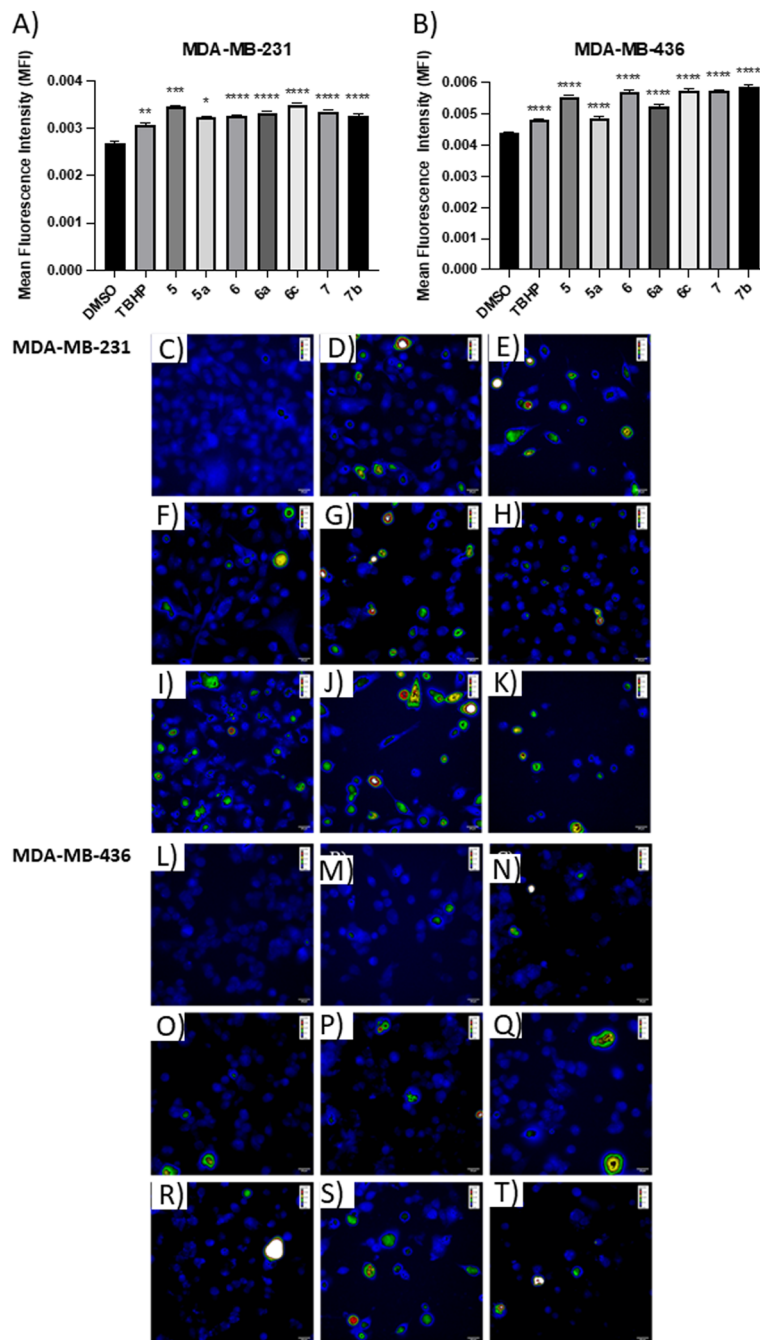


Fig. 5 Effect of compounds on intracellular ROS levels. Histograms display the quantification of mean fluorescence intensity (MFI) for vehicle or compounds in (A) MDA-MB-231 cells and (B) MDA-MB-436 cells. Representative confocal fluorescence microscopy images of ROS production in (C–K) MDA-MB-231 cells and (L–T) MDA-MB-436 cells. (C and L) 0.05% DMSO, (D and M) TBHP at 100 μ M, (E) **5** at 6.6 μ M, (F) **5a** at 25.5 μ M, (G) **6** at 5.5 μ M, (H) **6a** at 24.2 μ M, (I) **6c** at 9.6 μ M, (J) **7** at 11.1 μ M, (K) **7b** at 7.0 μ M, (N) **5** at 6.5 μ M, (O) **5a** at 15.5 μ M, (P) **6** at 9.7 μ M, (Q) **6a** at 15.6 μ M, (R) **6c** at 12.3 μ M, (S) **7** at 11.0 μ M, and (T) **7b** at 10.9 μ M. The data are expressed as the mean \pm SEM of three independent experiments performed in triplicate. * $P < 0.05$, ** $P < 0.01$, *** $P < 0.001$, **** $P < 0.0001$ vs. DMSO group.

capacity of the apoptotic and necrotic compounds (**5**, **6**, **6a**, **7**, and **7b**) to trigger oxidative stress was further studied in both cancer cell lines, whereas non-apoptotic but cytotoxic compounds (**5c**, **6b**, **7a**, and **7c** for both cancer cell lines, and **5b** for MDA-MB-231 cells) were studied to evaluate their influence on cell cycle distribution.

2.2.3. Measurement of reactive oxygen species (ROS) levels. At low or moderate doses, ROS are considered essential for the regulation of normal physiological cell conditions. However, high ROS levels cause damage to proteins, nucleic acids, lipids, membranes, and organelles, which can lead to the activation of cell death processes such as cell apoptosis.³² Because oxidative stress promotes apoptotic mechanisms, the effect of apoptotic benzopyrans in ROS production was evaluated. To that end, cell lines MDA-MB-231 and MDA-MB-436 were treated with selected representative apoptotic compounds at their respective IC₂₅ values. Then, fluorescence microscopy was employed to detect intracellular ROS levels by the dichlorodihydrofluorescein-diacetate (DCFDA) method.

The positive control, *tert*-butyl hydroperoxide (TBHP), significantly increased the mean fluorescence level, thus confirming its action mechanism. The results demonstrated that the apoptotic compounds **5**, **5a**, **6**, **6a**, **6c**, **7**, and **7b** significantly increased the level of ROS production in both TNBC cell lines (Fig. 5), as compared to control cells. The results suggested that these compounds can induce apoptosis by the generation of ROS in TNBC cells.

2.2.4. Cell cycle analysis. Because the cell growth inhibition observed in the cytotoxicity assay could be due to cell death *via* apoptosis/necrosis or cell cycle arrest, flow cytometry analysis was carried out to examine the arrest effects of non-apoptotic benzopyrans (**5b**, **5c**, **6b**, **7a**, and **7c**) on the cell cycle of both TNBC cell lines. For that purpose, cell lines MDA-MB-231 and MDA-MB-436 were treated with each compound at concentrations equal to their respective IC₅₀ values (Table 1), and then stained with PI.

The results showed that all non-apoptotic compounds significantly increased the percentage of the cells in the G1 phase, and lowered the percentage of the cells in the S phase. Regarding the MDA-MB-231 cell line, the percentage of the cells in the G1 phase increased from 49.81% for the control group to 63.02%, 63.73%, 56.12%, 62.18%, and 60.36% for compounds **5b**, **5c**, **6b**, **7a**, and **7c**, respectively (Fig. 6A and C–H). In the MDA-MB-436 cell line, the percentage of the cells in the G1 phase rose from 41.01% for the control group to 57.87%, 45.81%, 43.89%, and 55.78% for compounds **5c**, **6b**, **7a**, and **7c**, respectively (Fig. 6B and I–M). The percentage of the cells in the S phase in the MDA-MB-231 cell line decreased from 42.68% for the control group to 24.84%, 18.38%, 29.33%, 22.81%, and 23.05% for compounds **5b**, **5c**, **6b**, **7a**, and **7c**, respectively (Fig. 6A and C–H), and in MDA-MB-436 cells, decreased from 40.08% for the control group to 24.25%, 34.56%, 36.58%, and 30.13% for compounds **5c**, **6b**, **7a**, and **7c**, respectively (Fig. 6B and I–M). These results suggest that

non-apoptotic 2-aminopropyl benzopyrans **5b**, **5c**, **6b**, **7a**, and **7c** caused cell cycle arrest at the G1 phase.

2.2.5. Gene expression. Apoptosis is regulated by complex interactions between pro- and anti-apoptotic members of the B cell lymphoma-2 (Bcl-2) protein family.³³ Among the Bcl-2 family proteins, Bcl-2 promotes cell survival, while others can induce cell death.^{34–36} The cell cycle is regulated by a group of proteins known as cyclins, such as cyclin D1 (CCND1) or cyclin E2 (CCNE2), which regulate the progression from G1 to S phase.^{37–41} To explore the apoptosis and cell cycle arrest mechanism involved in the most promising compounds (those with a more appropriate SI value), we evaluated the gene expression of anti-apoptotic *Bcl-2* as well as *CCND1* and *CCNE2* in TNBC cells. The results showed that apoptotic compounds **5a**, **6a**, and **7b** downregulated *Bcl-2* (Fig. 7A and B), whereas compound **5b** downregulated the expression of the *CCND1* and *CCNE2* genes (Fig. 7C and D).

3. Conclusions

Three series of 2-aminopropyl benzopyran derivatives were synthesised (Scheme 1) and evaluated for their antitumor activity against the MDA-MB-231 and MDA-MB-436 TNBC cell lines. The SAR studies showed that the presence of an amino group (secondary, tertiary, or quaternary) in the structure seems to be essential for cytotoxicity in both TNBC cell lines, and its modification to a urea function renders the derivatives devoid of an anti-tumor effect. For the three series, the cytotoxic activity was as follows: *N*-methylated derivatives (tertiary amines) **5b**, **6b**, and **7b** > secondary amines **5**, **6**, and **7** > quaternary amine salts **5c**, **6c**, and **7c** > free phenolic derivatives **5a**, **6a**, and **7a**. In addition, **5a**, **5b**, **6a**, and **7b** displayed slight selectivity for tumor cells.

An apoptotic and necrotic effect was observed for benzopyrans **5**, **5a**, **5b**, **6**, **6a**, **6c**, **7**, and **7b** due to, at least in part, an increase in ROS generation, while **5b**, **5c**, **6b**, **7a**, and **7c** caused cell cycle arrest in the G1 phase. Further cell-based mechanistic studies revealed that the most promising compounds, **5a**, **6a**, and **7b**, downregulated the expression of *Bcl-2*, and **5b** downregulated the expression of cyclins *CCND1* and *CCND2*. Therefore, 2-aminopropyl benzopyrans emerge as new hits and can be used for designing new potential lead compounds in the development of useful agents against TNBC.

4. Experimental section

4.1. Chemistry

Electrospray ionization high-resolution mass spectrometry (ESI-HRMS) was performed using a TripleTOF™ 5600 liquid chromatography-tandem mass spectrometry (LC/MS/MS) System (AB SCIEX) (Toronto, Canada). LC-MS detection was performed using an ultra-high performance liquid chromatography (UHPLC) apparatus (Shimadzu, LCMS-8040)

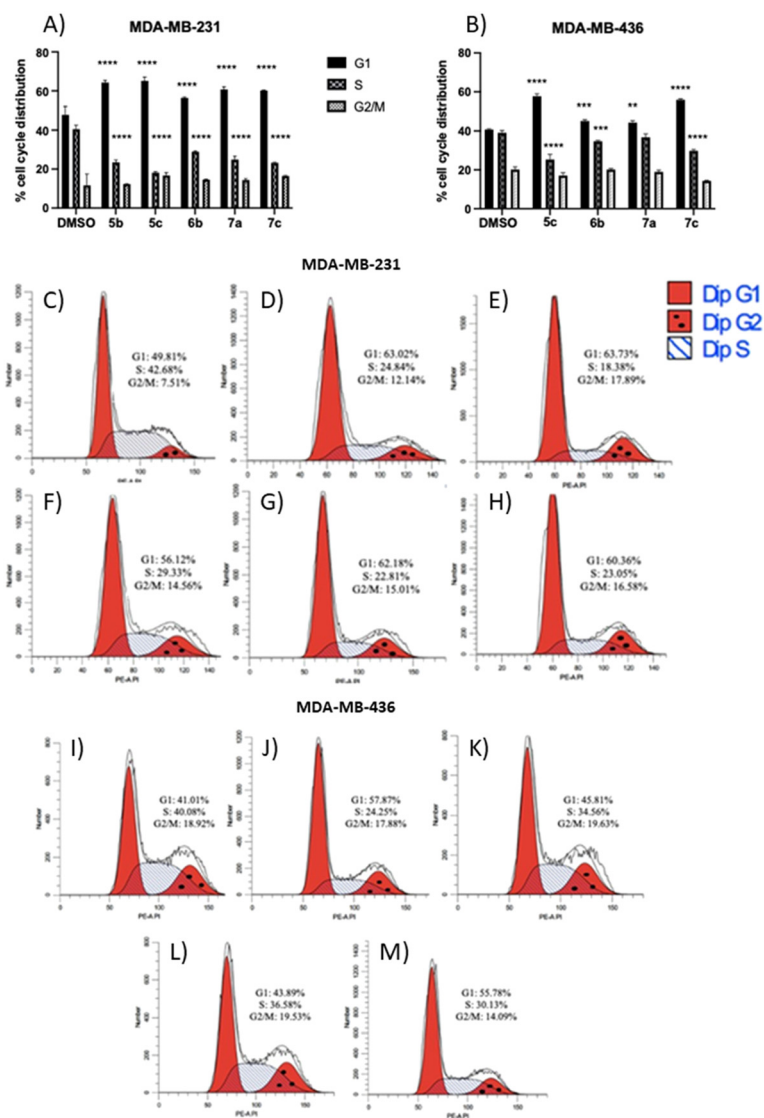


Fig. 6 Effect of non-apoptotic/necrotic compounds on cell cycle progression. The analysis of cell cycle distribution was performed by flow cytometry using PI staining. Histograms display the percentage of cell cycle distribution for (A) MDA-MB-231 cells and (B) MDA-MB-436 cells. Representative flow cytometry plots of cell cycle progression experiments with vehicle or non-apoptotic compounds for the (C–H) MDA-MB-231 cell line and (I–M) MDA-MB-436 cell line. (C and I) 0.1% DMSO, (D) **5b** at 7.3 μM , (E) **5c** at 25.0 μM , (F) **6b** at 1.5 μM , (G) **7a** at 58.4 μM , (H) **7c** at 42.2 μM , (J) **5c** at 24.0 μM , (K) **6b** at 2.0 μM , (L) **7a** at 55.2 μM , and (M) **7c** at 53.5 μM . The data are expressed as the mean \pm SD of three independent experiments performed in triplicate. ** $P < 0.01$, *** $P < 0.001$, **** $P < 0.0001$ vs. DMSO group.

coupled to a tandem mass spectrometry (MS/MS) triple quadrupole equipped with an ESI ion source (Shimadzu, Kyoto, Japan).

^1H NMR and ^{13}C NMR spectra were recorded on a Bruker AC-300 (Bruker Instruments, Kennewick, WA). The assignments in ^1H and ^{13}C NMR were made by correlation spectroscopy (COSY) 45, heteronuclear single quantum correlation (HSQC), and heteronuclear multiple bond correlation (HMBC) recorded at 300 MHz. Chemical shifts (δ) are reported in ppm relative to an internal deuterated solvent reference, with multiplicities indicated as s (singlet), d (doublet), t (triplet), q (quartet), m (multiplet), or dd (double doublet). All reactions were monitored by analytical thin-layer chromatography (TLC) with silica gel 60 F254 (Merck 5554).

Residues were purified by silica gel column chromatography (40–63 μm , Merck Group).

Solvents and reagents were purchased from the commercial sources Scharlab S.L. (Barcelona, Spain) and Sigma-Aldrich (St. Louis, MO, USA), respectively, and used without further purification unless otherwise noted. Dry and freshly distilled solvents were used in those reactions performed under N_2 . Quoted yields are of purified material. Final compounds were purified to $\geq 95\%$ as assessed by ^1H NMR and LC-MS/MS analysis.

Ethyl 3-(6-hydroxy-2-methyl-dihydrobenzopyran-2-yl)propanoate (1). Benzopyran ester **1** was synthesised as previously described^{27–30} from 2-(ethyl propanoate)-6-(hydroxyl)-2-(methyl)-dihydrobenzopyran-4-one. ^1H NMR (300 MHz,

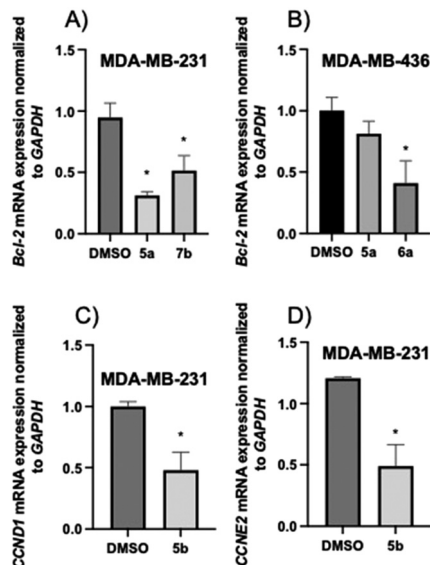


Fig. 7 Gene expression in TNBC cells treated with 2-aminopropyl benzopyrans **5a**, **5b**, **6a**, and **7b** at their respective IC_{25} values: (A) **5a** at 25.5 μ M and **7b** at 7.0 μ M, (B) **5a** at 15.5 μ M and **6a** at 15.6 μ M, and (C and D) **5b** at 3.7 μ M. The data are expressed as the mean \pm SD of three independent experiments performed in triplicate. * $P < 0.05$ vs. DMSO group.

$CDCl_3$) δ 6.59–6.53 (m, 3H, CH-5, CH-7, CH-8), 4.12 (q, $J = 7.1$ Hz, 2H, $CO_2CH_2CH_3$), 2.70 (m, 2H, CH_2-4), 2.44 (t, $J = 7.7$ Hz, 2H, CH_2-2'), 2.05–1.70 (m, 4H, CH_2-3 , CH_2-1'), 1.24 (t, $J = 7.1$ Hz, 3H, $CO_2CH_2CH_3$), 1.23 (s, 3H, CH_3-2); ^{13}C NMR (75 MHz, $CDCl_3$) δ 174.1 ($CO_2CH_2CH_3$), 148.8 (C-6), 147.4 (C-8a), 121.6 (C-4a), 117.8 (CH-5), 115.4 (CH-7), 114.6 (CH-8), 74.6 (C-2), 60.5 ($CO_2CH_2CH_3$), 34.3 (CH_2-1'), 31.1 (CH_2-3), 28.8 (CH_2-2'), 23.7 (CH_3-2), 22.1 (CH_2-4), 14.1 ($CO_2CH_2CH_3$); HREIMS m/z calculated for $C_{15}H_{20}O_4$ [M] $^+$ 264.1362, found: 264.1356.

Ethyl 3-(6-(*p*-fluorobenzoyloxy)-2-methyldihydrobenzopyran-2-yl)propanoate (2). A solution of benzopyran ester **1** (1.5 g, 5.68 mmol), *p*-fluorobenzyl chloride (0.9 mL, 7.38 mmol), and anhydrous K_2CO_3 (1.2 g, 8.49 mmol) in absolute EtOH (20 mL) was refluxed under N_2 for 4 hours. The mixture was evaporated, water was added (20 mL), and extraction proceeded with dichloromethane (3 \times 15 mL). The organic layers were washed with 1 M HCl and brine, dried over anhydrous Na_2SO_4 , and evaporated under reduced pressure. The residue was purified by column chromatography (hexane/EtOAc, 90:10) to yield the *O*-protected benzopyran ester (**2**) (1.7 g, 79%) as a colorless oil. 1H NMR (300 MHz, $CDCl_3$) δ 7.41–7.36 (m, 2H, CH-2'', CH-6''), 7.09–7.03 (m, 2H, CH-3'', CH-5''), 6.72–6.67 (m, 3H, CH-5, CH-7, CH-8), 4.94 (s, 2H, $OCH_2Ph-p-F$), 4.13 (q, $J = 7.1$ Hz, 2H, $CO_2CH_2CH_3$), 2.76 (t, $J = 6.7$ Hz, 2H, CH_2-4), 2.48 (t, $J = 7.7$ Hz, 2H, CH_2-2'), 2.0–1.75 (m, 4H, CH_2-3 , CH_2-1'), 1.24 (t, $J = 7.2$ Hz, 3H, $CO_2CH_2CH_3$), 1.23 (s, 3H, CH_3-2); ^{13}C NMR (75 MHz, $CDCl_3$) δ 173.6 ($CO_2CH_2CH_3$), 162.3 (d, $J_{CF} = 244$ Hz, C-4''), 152.0 (C-6), 147.9 (C-8a), 133.1 (d, $J_{CF} = 3$ Hz, C-1''), 129.1 (d, $J_{CF} = 8$ Hz, CH-2'', CH-6''), 121.4 (C-4a), 117.7 (CH-5), 115.2 (d, $J_{CF} = 25$ Hz, CH-3'', CH-5''), 115.1 (CH-7), 114.4

(CH-8), 74.6 (C-2), 69.9 ($OCH_2Ph-p-F$), 60.3 ($CO_2CH_2CH_3$), 34.3 (CH_2-1'), 31.0 (CH_2-3), 28.7 (CH_2-2'), 23.6 (CH_3-2), 22.2 (CH_2-4), 14.1 ($CO_2CH_2CH_3$); HREIMS m/z calculated for $C_{22}H_{25}O_4F$ [M] $^+$ 372.1737, found: 372.1730.

3-(6-(*p*-Fluorobenzoyloxy)-2-methyldihydrobenzopyran-2-yl)propanal (3). A solution of **2** (500 mg, 1.34 mmol) in dry dichloromethane (10 mL) at -78 $^\circ C$ under nitrogen atmosphere was stirred for 10 minutes. To this solution was added dropwise 8.8 mL of 1.0 M DIBAL-H solution in tetrahydrofuran (THF). After 15 minutes, the mixture was quenched by addition of 5 mL of MeOH and 10 mL of half sat aqueous NH_4Cl solution. The reaction mixture was stirred for an additional 10 minutes at room temperature, and then was concentrated *in vacuo*. Then, water was added (15 mL), and extraction proceeded with EtOAc (3 \times 15 mL). The organic layers were washed with brine, dried over anhydrous Na_2SO_4 , and evaporated under reduced pressure. The residue was purified by silica gel column chromatography (hexane/EtOAc, 90:10) to afford 492 mg of the corresponding aldehyde **3** (406 mg, 92%) as a colorless oil. 1H NMR (300 MHz, $CDCl_3$) δ 9.78 (t, $J = 1.6$ Hz, 1H, CHO), 7.39–7.37 (m, 2H, H-2'', H-6''), 7.08–7.04 (m, 2H, H-3'', H-5''), 6.74–6.67 (m, 3H, H-5, H-7, H-8), 4.94 (s, 2H, $OCH_2Ph-p-F$), 2.77–2.74 (m, 2H, CH_2-4), 2.62–2.59 (m, 2H, CH_2-2'), 2.03–1.75 (m, 4H, CH_2-3 , CH_2-1'), 1.26 (s, 3H, CH_3-2); ^{13}C NMR (75 MHz, $CDCl_3$) δ 202.2 (CHO), 162.4 (d, $J_{CF} = 244$ Hz, C-4''), 152.1 (C-6), 147.7 (C-8a), 133.1 (d, $J_{CF} = 3$ Hz, C-1''), 129.3 (d, $J_{CF} = 8$ Hz, C-2'', C-6''), 121.4 (C-4a), 117.7 (CH-5), 115.2 (d, $J_{CF} = 25$ Hz, CH-3'', CH-5''), 115.2 (CH-7), 114.5 (CH-8), 74.6 (C-2), 69.9 ($OCH_2Ph-p-F$), 38.4 (CH_2-2'), 31.8 (CH_2-1'), 31.2 (CH_2-3), 23.7 (CH_3-2), 22.3 (CH_2-4); HRMS (ESI) m/z calculated for $C_{20}H_{21}O_3F$ [$M + H$] $^+$ 329.1547, found: 329.1552.

(*N*-3,4-Dimethoxyphenethyl)-3-(6-(*p*-fluorobenzoyloxy)-2-methyldihydrobenzopyran-2-yl)propanamide (4). A solution of ester **2** (1 g, 3.05 mmol) was dissolved in dry MeOH (10 mL) and KOH 20% (5 mL), and was refluxed under N_2 for 4 hours. The mixture was evaporated, water was added (20 mL), and extraction proceeded with dichloromethane (3 \times 15 mL). The organic layers were washed with 1 M HCl and brine, dried over anhydrous Na_2SO_4 , and evaporated under reduced pressure to obtain 980 mg of carboxylic acid. To a solution of the carboxylic acid (980 mg, 2.85 mmol), dry dichloromethane and $SOCl_2$ (1.6 mL, 22.8 mmol) were added, and the solution was then reacted under reflux and N_2 for 3 hours. After stirring for an additional 30 minutes at room temperature, water was added (20 mL), and extraction proceeded with dichloromethane (3 \times 15 mL). The organic layers were washed with brine, dried over anhydrous Na_2SO_4 , and evaporated under reduced pressure to obtain 1.3 g of chloride acid. A mixture of 3,4-dimethoxyphenethylamine (1.2 mL, 6.9 mmol), 4-DMAP (200 mg, 1.64 mmol), and Et_3N (0.06 mL, 0.45 mmol) was dissolved in 1 mL of dry dichloromethane under N_2 . To this mixture, a solution of the acid chloride (1 g, 2.6 mmol) in dry dichloromethane was added dropwise. This reaction remained at room temperature and under N_2 overnight. Dichloromethane (3 \times 15 mL) was

added to the reaction mixture, and the organic layer was washed with HCl 1 M and brine, dried with anhydrous Na₂SO₄, filtered, and then evaporated to dryness. The residue obtained was subjected to silica gel column chromatography (hexane/EtOAc, 60:40) to afford compound 4 (976 mg, 63% yield) as a white oil. ¹H NMR (300 MHz, CDCl₃) δ 7.41–7.33 (m, 2H, CH-2'', CH-6''), 7.08–7.02 (m, 2H, CH-3'', CH-5''), 6.80–6.62 (m, 6H, CH-5, CH-7, CH-8, CH-2''', CH-5''', CH-6'''), 5.69 (s, NH), 4.92 (s, 2H, OCH₂Ph-*p*-F), 3.85 (s, 6H, 2xOCH₃), 3.48–3.45 (m, 2H, CH₂-α), 2.81–2.67 (m, 4H, CH₂-4, CH₂-β), 2.32–2.27 (CH₂-2'), 2.03–1.83 (m, 2H, CH₂-1'), 1.80–1.67 (m, 2H, CH₂-3), 1.25 (s, 3H, CH₃-2). ¹³C NMR (75 MHz, CDCl₃) δ 172.9 (C=O), 162.0 (d, *J*_{CF} = 244 Hz, C-4''), 158.3 (C-3''', C-4'''), 152.1 (C-6), 147.9 (C-8a), 133.2 (d, *J*_{CF} = 3 Hz, C-1''), 130.9 (C-1'''), 129.7 (CH-6'''), 129.3 (d, *J*_{CF} = 8 Hz, CH-2'', CH-6''), 121.6 (C-4a), 117.5 (CH-5), 115.4 (d, *J*_{CF} = 21 Hz, CH-3'', CH-5''), 115.2 (CH-7), 114.5 (CH-8), 114.1 (CH-2''', CH-5'''), 75.0 (C-2), 70.0 (OCH₂Ph-*p*-F), 55.3 (2xOCH₃), 40.8 (CH₂-α), 35.2 (CH₂-1'), 34.8 (CH₂-β), 31.2 (CH₂-3), 30.8 (CH₂-2'), 23.7 (CH₃-2), 22.3 (CH₂-4). HRMS (ESI) *m/z* calculated for C₃₀H₃₅FNO₅ [M + H]⁺ 508.2494, found: 508.2481.

General procedure for synthesis of amine benzopyrans 5 and 6. A mixture of aldehyde 3 (240 mg, 0.73 mmol) and 4-methoxy-phenethylamine (0.25 mL, 1.4 mmol) or 2,2-diphenylethylamine (237 mg, 1.2 mmol) was dissolved in 5 mL of dry dichloroethane. The mixture was stirred at room temperature for 15 minutes and then added to a solution of sodium triacetoxylborohydride (360 mg, 1.7 mmol) and a drop of acetic acid in 1 mL of dry dichloroethane. The mixtures were stirred at room temperature under N₂ for 1 hour. Reaction mixtures were extracted with EtOAc (3 × 10 mL). The organic layer was washed with water and brine, dried with anhydrous Na₂SO₄, filtered, and then evaporated to dryness. The residue obtained was subjected to silica gel column chromatography (CH₂Cl₂/MeOH, 98:2) to afford compound 5 (244 mg, 72% yield) or 6 (201 mg, 54% yield) as colorless oils.

3-(6-(*p*-Fluorobenzyloxy)-2-methyldihydrobenzopyran-2-yl)-*N*-(*p*-methoxyphenethyl)propanamine (5). ¹H NMR (300 MHz, CDCl₃) δ 7.36–7.32 (m, 2H, CH-2'', CH-6''), 7.08–6.98 (m, 4H, CH-3'', CH-5'', CH-2''', CH-6'''), 6.82–6.78 (m, 2H, CH-3''', CH-5'''), 6.68–6.60 (m, 3H, CH-5, CH-7, CH-8), 4.89 (s, 2H, OCH₂-Ph-*p*-F), 3.74 (s, 3H, OCH₃), 3.03–2.57 (m, 8H, CH₂-4, CH₂-3', CH₂-α, CH₂-β), 1.78–1.66 (m, 2H, CH₂-3), 1.59–1.50 (m, 4H, CH₂-1', CH₂-2'), 1.20 (s, 3H, CH₃-2). ¹³C NMR (75 MHz, CD₃-OD) δ 162.0 (d, *J*_{CF} = 244 Hz, C-4''), 159.0 (C-4'''), 152.2 (C-6), 147.7 (C-8a), 133.7 (CH-1''), 129.4 (CH-2'', CH-6'''), 129.2 (d, *J*_{CF} = 8 Hz, CH-2'', CH-6''), 128.1 (C-1'''), 121.6 (C-4a), 117.3 (CH-5), 115.0 (CH-7), 114.9 (CH-3''', CH-5'''), 114.5 (d, *J*_{CF} = 13 Hz, CH-3'', CH-5''), 114.0 (CH-8), 74.9 (C-2), 69.6 (OCH₂Ph-*p*-F), 54.4 (OCH₃), 48.7 (CH₂-3', CH₂-α), 35.7 (CH₂-1'), 31.1 (CH₂-3), 30.8 (CH₂-β), 22.6 (CH₃-2), 21.8 (CH₂-4), 20.2 (CH₂-2'). HRMS (ESI) *m/z* calculated for C₂₉H₃₄FNO₃ [M + H]⁺ 464.2595, found: 464.2581.

***N*-(2,2-Diphenylethyl)-3-(6-(*p*-fluorobenzyloxy)-2-methyldihydrobenzopyran-2-yl)propanamine (6).** ¹H NMR

(300 MHz, CDCl₃) δ 7.44–7.40 (m, 2H, CH-2'', CH-6''), 7.36–7.22 (m, 10H, 2xPh), 7.15–7.08 (m, 2H, CH-3'', CH-5''), 6.80–6.71 (m, 3H, CH-5, CH-7, CH-8), 4.99 (s, 2H, OCH₂Ph-*p*-F), 4.28 (t, 1H, *J* = 7.8 Hz, CH-β), 3.30 (d, 2H, *J* = 7.8 Hz, CH₂-α), 2.76–2.70 (m, 4H, CH₂-4, CH₂-3'), 1.80–1.73 (m, 2H, CH₂-3), 1.65–1.54 (m, 4H, CH₂-1', CH₂-2'), 1.26 (s, 3H, CH₃-2). ¹³C NMR (75 MHz, CDCl₃) δ 162.5 (d, *J*_{CF} = 244 Hz, C-4''), 151.9 (C-6), 148.0 (C-8a), 142.5 (C-Ph), 133.2 (d, *J*_{CF} = 3 Hz, C-1''), 129.2 (d, *J*_{CF} = 8 Hz, CH-2'', CH-6''), 128.7 and 128.0 (CH-Ph), 121.6 (C-4a), 117.7 (CH-5), 115.3 (d, *J*_{CF} = 22 Hz, CH-3'', CH-5''), 115.2 (CH-7), 114.4 (CH-8), 75.3 (C-2), 70.0 (OCH₂Ph-*p*-F), 53.9 (CH₂-α), 50.7 (CH-β), 49.8 (CH₂-3'), 36.9 (CH₂-1'), 30.9 (CH₂-3), 23.9 (CH₃-2), 23.5 (CH₂-2'), 22.3 (CH₂-4). HRMS (ESI) *m/z* calculated for C₃₄H₃₆FNO₂ [M + H]⁺ 510.2803, found: 510.2801.

General procedure for synthesis of amine benzopyran 7. A mixture of amide 4 (880 mg, 1.72 mmol) and phosphoryl chloride (2.4 mL, 26 mmol) was dissolved in dry dichloromethane (10 mL) and refluxed under N₂ overnight. The reaction mixture was evaporated to dryness and dissolved in dry MeOH (7 mL) in an ice bath at –78 °C. Sodium borohydride (600 mg, 15.9 mmol) was added, and the reaction remained at room temperature and under N₂ for 2 hours. Then, the reaction mixture was alkalinized with ammonia 5% and extracted with EtOAc (3 × 15 mL). The organic layer was washed with water and brine, dried with anhydrous Na₂SO₄, filtered, and evaporated to dryness. The residue obtained was subjected to silica gel column chromatography (CH₂Cl₂/MeOH, 98:2) to afford compound 7 (443.8 mg, 53% yield) as a colorless oil.

1-(2-(6-((4-Fluorobenzyl)oxy)-2-methyldihydrobenzopyran-2-yl)ethyl)-6,7-dimethoxy-1,2,3,4-tetrahydroisoquinoline (7). ¹H NMR (300 MHz, CDCl₃) δ 7.41–7.35 (m, 2H, CH-2'', CH-6''), 7.10–7.02 (m, 2H, CH-3'', CH-5''), 6.74–6.58 (m, 3H, CH-5, CH-7, CH-8), 6.56 and 6.55 (2 s, 2H, CH-2''', CH-5'''), 4.93 (s, 2H, OCH₂Ph-*p*-F), 3.99–3.95 (m, 1H, CH-3'), 3.84 and 3.77 (2 s, 6H, 2xOCH₃), 3.25–3.18 and 2.99–2.94 (2 m, 2H, CH₂-α), 2.93–2.65 (m, 4H, CH₂-4, CH₂-β), 1.99–1.67 (m, 6H, CH₂-3, CH₂-1', CH₂-2'), 1.28 (s, 3H, CH₃-2). ¹³C NMR (75 MHz, CDCl₃) δ 162.0 (d, *J*_{CF} = 244 Hz, C-4''), 152.0 (C-6), 148.2 (C-8a), 147.5 and 147.3 (C-3''', C-4'''), 133.2 (d, *J*_{CF} = 3 Hz, C-1''), 129.3 (d, *J*_{CF} = 8 Hz, CH-2'', CH-6''), 127.0 (C-1''', C-6'''), 121.7 (C-4a), 117.7 (CH-5), 115.5 (d, *J*_{CF} = 21 Hz, CH-3'', CH-5''), 115.2 (CH-7), 114.4 (CH-8), 111.8 (CH-2'''), 109.2 (CH-5'''), 75.7 (C-2), 70.0 (OCH₂Ph-*p*-F), 56.0 and 55.8 (2xOCH₃), 55.9 (CH-3'), 41.1 (CH₂-α), 35.5 (CH₂-1'), 31.4 (CH₂-3), 30.9 (CH₂-2'), 29.6 (CH₂-β), 24.2 (CH₃-2), 22.5 (CH₂-4). HRMS (ESI) *m/z* calculated for C₃₀H₃₄FNO₄ [M + H]⁺ 492.2545, found: 492.2523.

General procedure for O-deprotection to prepare compounds 5a, 6a, and 7a. Amine 5 (50 mg, 0.11 mmol), 6 (56 mg, 0.11 mmol), and 7 (54 mg, 0.11 mmol) was dissolved in 1 M HCl:EtOH in a 1:1 ratio, and refluxed under N₂ for 3 hours. Reaction mixtures were stirred for an additional 30 minutes at room temperature, and ammonia 15% was added for alkalinization. Mixtures were concentrated *in vacuo*, and then, water was added, and extraction proceeded with EtOAc (3 × 15 mL). The combined organic layers were dried over

anhydrous Na₂SO₄ and evaporated to dryness. The residue was purified by C18 column chromatography to afford 36.1 mg, 42.5 mg, and 40.6 mg of the corresponding compound **5a**, **6a**, and **7a** (92–96%) as colorless oils.

3-(6-Hydroxy-2-methylidihydrobenzopyran-2-yl)-N-(*p*-methoxyphenethyl)propanamine (5a). ¹H NMR (300 MHz, CD₃OD) δ 7.20 (d, 2H, *J* = 8.6 Hz, CH-2'', CH-6''), 6.90 (d, 2H, *J* = 8.6 Hz, CH-3''', CH-5'''), 6.53–6.50 (m, 3H, CH-5, CH-7, CH-8), 3.78 (s, 3H, OCH₃), 3.22–2.89 (m, 6H, CH₂-3', CH₂-α, CH₂-β), 2.77–2.71 (m, 2H, CH₂-4), 1.92–1.56 (m, 6H, CH₂-3, CH₂-1', CH₂-2'), 1.27 (s, 3H, CH₃-2). ¹³C NMR (75 MHz, CD₃OD) δ 160.6 (C-4''), 151.7 (C-6), 148.0 (C-8a), 131.0 (CH-2'', CH-6''), 129.7 (C-1''), 123.1 (C-4a), 118.7 (CH-5), 116.4 (CH-3''', CH-5'''), 115.7 (CH-7), 115.6 (CH-8), 76.1 (C-2), 55.9 (OCH₃), 50.6 (CH₂-3', CH₂-α), 37.2 (CH₂-1'), 32.8 (CH₂-3), 32.6 (CH₂-β), 24.2 (CH₃-2), 23.3 (CH₂-4), 21.9 (CH₂-2'). HRMS (ESI) *m/z* calculated for C₂₂H₂₉NO₃ [M + H]⁺ 356.2220, found: 356.2217.

2-(3-((2,2-Diphenylethyl)amino)propyl)-2-methylidihydrobenzopyran-6-ol (6a). ¹H NMR (300 MHz, CDCl₃) δ 7.30–7.20 (m, 10H, 2*xPh*), 6.55–6.47 (m, 3H, CH-5, CH-7, CH-8), 4.23 (t, *J* = 7.7 Hz, 1H, CH-β), 3.24 (d, *J* = 7.7 Hz, 2H, CH₂-α), 2.68–2.56 (m, 4H, CH₂-4, CH₂-3'), 1.70–1.45 (m, 6H, CH₂-3, CH₂-1', CH₂-2'), 1.19 (s, 3H, CH₃-2). ¹³C NMR (75 MHz, CDCl₃) δ 149.2 (C-6), 147.2 (C-8a), 142.4 (C-Ph), 128.7, 128.0 and 126.7 (2XCH-Ph), 121.7 (C-4a), 117.7 (CH-5), 115.6 (CH-7), 114.8 (CH-8), 75.3 (C-2), 54.0 (CH₂-α), 50.6 (CH-β), 49.8 (CH₂-3'), 36.7 (CH₂-1'), 30.9 (CH₂-3), 24.0 (CH₃-2), 23.5 (CH₂-2'), 22.2 (CH₂-4). HRMS (ESI) *m/z* calculated for C₂₇H₃₁NO₂ [M + H]⁺ 402.2428, found: 402.2417.

2-(2-(6,7-Dimethoxy-1,2,3,4-tetrahydroisoquinolin-1-yl)ethyl)-2-methylidihydrobenzopyran-6-ol (7a). ¹H NMR (300 MHz, CDCl₃ + 1 drop CD₃OD) δ 6.51–6.44 (m, 5H, CH-5, CH-7, CH-8, CH-2'', CH-5''), 4.10–4.01 (m, 1H, CH-3'), 3.75 (s, 6H, 2xOCH₃), 3.28–3.20 and 3.02–2.88 (2 m, 2H, CH₂-α), 2.85–2.55 (m, 4H, CH₂-4, CH₂-β), 1.97–1.93 (m, 1H, CH₂-3), 1.72–1.63 (m, 4H, CH₂-1', CH₂-2'), 1.19 (s, 3H, CH₃-2). ¹³C NMR (75 MHz, CDCl₃ + 1 drop CD₃OD) δ 149.8 (C-6), 148.1 (C-8a), 147.7 (C-3'', C-4''), 127.1 (C-1'', C-6''), 121.8 (C-4a), 117.5 (CH-5), 115.4 (CH-7), 114.5 (CH-8), 111.6 and 109.1 (CH-2'', CH-5''), 75.2 (C-2), 55.9 (CH-3'), 55.2 and 55.1 (2xOCH₃), 40.1 (CH₂-α), 35.0 (CH₂-1'), 31.3 (CH₂-3), 29.5 (CH₂-β), 28.6 (CH₂-2'), 23.6 (CH₃-2), 22.1 (CH₂-4). HRMS (ESI) *m/z* calculated for C₂₃H₂₉NO₄ [M + H]⁺ 384.2169, found: 384.2169.

General procedure for synthesis of *N*-methylated amines 5b, 6b, and 7b. A mixture of **5** (50 mg, 0.11 mmol), **6** (56 mg, 0.11 mmol), and **7** (54 mg, 0.11 mmol), formaldehyde (1 mL), and formic acid (two drops) was dissolved in MeOH (10 mL). The reaction was refluxed under N₂ for 1 hour. The reaction mixture was stirred for an additional 30 minutes at room temperature. Then, sodium borohydride (50 mg, 1.3 mmol) was added, and the reaction mixture was stirred for 45 minutes, and then basified by Et₃N. Water was added (10 mL), and the mixture was extracted with EtOAc (3 × 10 mL). The combined organic layers were dried over anhydrous Na₂SO₄ and evaporated to dryness. The residue was purified by

silica gel column chromatography (CH₂Cl₂/MeOH, 98:2) to afford 40 mg, 46 mg, and 47.9 mg of **5b**, **6b**, and **7b**, respectively, (76–86% yield) as colorless oils.

3-(6-(*p*-Fluorobenzyloxy)-2-methylidihydrobenzopyran-2-yl)-N-(*p*-methoxyphenethyl)-*N*-methylpropanamine (5b). ¹H NMR (300 MHz, CDCl₃) δ 7.41–7.36 (m, 2H, CH-2'', CH-6''), 7.12–7.03 (m, 4H, CH-3''', CH-5''', CH-2''', CH-5'''), 6.85–6.81 (m, 2H, CH-3''', CH-5'''), 6.74–6.66 (m, 3H, CH-5, CH-7, CH-8), 4.94 (s, 2H, OCH₂Ph-*p*-F), 3.80 (s, 3H, OCH₃), 2.78–2.73 (m, 4H, CH₂-3', CH₂-β), 2.71–2.70 (m, 2H, CH₂-4), 2.67–2.59 (m, 2H, CH₂-α), 2.34 (s, 3H, NCH₃), 1.82–1.55 (m, 6H, CH₂-3, CH₂-1', CH₂-2'), 1.26 (s, 3H, CH₃-2). ¹³C NMR (75 MHz, CDCl₃) δ 162.6 (d, *J*_{CF} = 244 Hz, C-4''), 158.0 (C-4''), 151.9 (C-6), 148.2 (C-8a), 133.2 (d, *J*_{CF} = 3 Hz, C-1''), 132.0 (C-1''), 129.6 (CH-2'', CH-6''), 129.3 (d, *J*_{CF} = 8 Hz, CH-2'', CH-6''), 121.7 (C-4a), 117.7 (CH-5), 115.4 (d, *J*_{CF} = 21 Hz, CH-3''', CH-5'''), 115.2 (CH-7), 114.4 (CH-8), 113.8 (CH-3''', CH-5'''), 75.6 (C-2), 70.0 (OCH₂Ph-*p*-F), 59.5 (CH₂-3'), 57.7 (CH₂-α), 55.2 (OCH₃), 41.9 (NCH₃), 37.1 (CH₂-1'), 32.5 (CH₂-3), 31.0 (CH₂-β), 24.0 (CH₃-2), 22.4 (CH₂-4), 21.0 (CH₂-2'). HRMS (ESI) *m/z* calculated for C₃₀H₃₆FNO₃ [M + H]⁺ 478.2752, found: 478.2744.

***N*-(2,2-Diphenylethyl)-3-(6-(*p*-fluorobenzyloxy)-2-methylidihydrobenzopyran-2-yl)-*N*-methylpropan-1-amine (6b).** ¹H NMR (300 MHz, CDCl₃) δ 7.43–7.39 (m, 2H, CH-2'', CH-6''), 7.29–7.15 (m, 10H, 2*xPh*), 7.10–7.05 (m, 2H, CH-3''', CH-5'''), 6.75–6.68 (m, 3H, CH-5, CH-7, CH-8), 4.96 (s, 2H, OCH₂Ph-*p*-F), 4.16 (t, *J* = 7.0 Hz, 1H, CH-β), 2.98 (d, *J* = 7.0 Hz, 2H, CH₂-α), 2.65–2.64 (m, 2H, CH₂-4), 2.42–2.38 (m, 2H, CH₂-3'), 2.25 (s, 3H, NCH₃), 1.82–1.65 (m, 2H, CH₂-3), 1.56–1.41 (m, 4H, CH₂-1', CH₂-2'), 1.23 (s, 3H, CH₃-2). ¹³C NMR (75 MHz, CDCl₃) δ 162.0 (d, *J*_{CF} = 244 Hz, C-4''), 151.9 (C-6), 148.3 (C-8a), 143.8 (C-Ph), 133.2 (d, *J*_{CF} = 2 Hz, CH-1''), 129.3 (d, *J*_{CF} = 8 Hz, CH-2'', CH-6''), 128.3 and 126.2 (CH-Ph), 121.8 (C-4a), 117.8 (CH-5), 115.2 (d, *J*_{CF} = 21 Hz, CH-3''', CH-5'''), 115.2 (CH-7), 114.4 (CH-8), 75.7 (C-2), 70.1 (OCH₂Ph-*p*-F), 62.7 (CH₂-α), 58.4 (CH₂-3'), 49.5 (CH-β), 42.5 (NCH₃), 37.1 (CH₂-1'), 31.0 (CH₂-3), 24.1 (CH₃-2), 22.5 (CH₂-4), 21.0 (CH₂-2'). HRMS (ESI) *m/z* calculated for C₃₅H₃₈FNO₂ [M + H]⁺ 524.2959, found: 524.2945.

1-(2-(6-(*p*-Fluorobenzyloxy)-2-methylidihydrobenzopyran-2-yl)ethyl)-6,7-dimethoxy-2-methyl-1,2,3,4-tetrahydroisoquinoline (7b). ¹H NMR (300 MHz, CDCl₃) δ 7.41–7.36 (m, 2H, CH-2'', CH-6''), 7.08–7.03 (m, 2H, CH-3''', CH-5'''), 6.73–6.61 (m, 3H, CH-5, CH-7, CH-8), 6.55 and 6.54 (2 s, 2H, CH-2'', CH-5''), 4.93 (s, 2H, OCH₂Ph-*p*-F), 3.84 and 3.83 (m, 6H, 2xOCH₃), 3.58–3.51 (m, 1H, CH-3'), 3.43–3.37 and 3.12–3.06 (2 m, 2H, CH₂-α), 2.73–2.64 (m, 4H, CH₂-4, CH₂-β), 2.40 (s, 3H, NCH₃), 1.95–1.90 (m, 2H, CH₂-3), 1.82–1.56 (m, 4H, CH₂-1', CH₂-2'), 1.26 (s, CH₃-2). ¹³C NMR (75 MHz, CDCl₃) δ 162 (d, *J*_{CF} = 244 Hz, C-4''), 151.9 (C-6), 148.3 (C-8a), 147.3 (C-3''', C-4''), 133.3 (d, *J*_{CF} = 3 Hz, C-1''), 129.4 (d, *J*_{CF} = 8 Hz, CH-2'', CH-6''), 126.9 (C-1'', C-6''), 121.8 (C-4a), 117.7 (CH-5), 115.4 (d, *J*_{CF} = 21 Hz, CH-3''', CH-5'''), 115.2 (CH-7), 114.4 (CH-8), 111.3 (CH-2''), 109.8 (CH-5''), 75.8 (C-2), 70.0 (OCH₂Ph-*p*-F), 63.4 (CH-3'), 55.9 and 55.8 (OCH₃), 49.1 (CH₂-α), 42.8 (NCH₃), 34.7 (CH₂-1'), 30.9 (CH₂-3), 29.7 (CH₂-2'), 27.8 (CH₂-β), 24.2 (CH₃-2),

22.5 (CH₂-4). HRMS (ESI) *m/z* calculated for C₃₁H₃₆FNO₄ [M + H]⁺ 506.2701, found: 506.2705.

General procedure for synthesis of *N*-dimethylated amines 5c, 6c, and 7c. A mixture of 5 (50 mg, 0.11 mmol), 6 (56 mg, 0.11 mmol), 7 (54 mg, 0.11 mmol), and methyl iodide (1.5 mL) was dissolved in dimethylformamide (8 mL) and refluxed under N₂ for 30 minutes to 1 hour. Reaction mixtures were extracted with EtOAc (3 × 10 mL). The organic layer was extracted with water and brine, dried with anhydrous Na₂SO₄, filtered, and evaporated to dryness. The residue obtained was subjected to silica gel column chromatography (CH₂Cl₂/MeOH, 95:5) to afford 42.8 mg, 47.4 mg, and 55 mg of the respective compounds 5c, 6c, and 7c (79–96% yield) as brown oils.

3-(6-(*p*-Fluorobenzyloxy)-2-methylidihydrobenzopyran-2-yl)-*N*-(*p*-methoxyphenethyl)-*N,N*-dimethylpropan-1-aminium (5c). ¹H NMR (300 MHz, CDCl₃) δ 7.41–7.36 (m, 2H, CH-2'', CH-6''), 7.25–7.18 (m, 2H, H-2''', H-6'''), 7.10–7.01 (m, 2H, CH-3'', CH-5''), 6.91–6.87 (m, 2H, CH-3''', CH-5'''), 6.73–6.67 (m, 3H, CH-5, CH-7, CH-8), 4.94 (s, 2H, OCH₂Ph-*p*-F), 3.78 (s, 3H, OCH₃), 3.59–3.45 (m, 4H, CH₂-α, CH₂-3'), 3.26 (s, N(CH₃)₂), 3.09–3.03 (m, 2H, CH₂-β), 2.80–2.76 (m, 2H, CH₂-4), 2.17–1.68 (m, 6H, CH₂-3, CH₂-1', CH₂-2'), 1.32 (s, 3H, CH₃-2). ¹³C NMR (75 MHz, CDCl₃) δ 162.4 (d, *J*_{CF} = 245 Hz, C-4''), 159.2 (C-4'''), 152.4 (C-6), 147.5 (C-8a), 133.1 (d, *J*_{CF} = 3 Hz, C-1''), 130.2 (CH-2''', CH-6'''), 129.3 (d, *J*_{CF} = 9 Hz, CH-2'', CH-6''), 129.3 (C-1'''), 121.7 (C-4a), 117.6 (CH-5), 115.4 (d, *J*_{CF} = 21 Hz, CH-3'', CH-5''), 115.4 (CH-7), 114.9 (CH-3''', CH-5'''), 114.7 (CH-8), 75.0 (C-2), 70.0 (OCH₂-Ph-*p*-F), 65.8 (CH₂-α), 65.5 (CH₂-3'), 55.4 (OCH₃), 52.3 (N(CH₃)₂), 36.0 (CH₂-1'), 31.9 (CH₂-3), 30.9 (CH₂-β), 23.9 (CH₃-2), 22.7 (CH₂-4), 17.4 (CH₂-2'). HRMS (ESI) *m/z* calculated for C₃₁H₃₈FNO₃ [M + H]⁺ 492.2908, found: 492.2895.

***N*-(2,2-Diphenylethyl)-3-(6-(*p*-fluorobenzyloxy)-2-methylidihydrobenzopyran-2-yl)-*N,N*-dimethylpropan-1-aminium (6c).** ¹H NMR (300 MHz, CDCl₃) δ 7.48–7.40 (m, 2H, CH-2'', CH-6''), 7.39–7.21 (m, 10H, 2*x*Ph), 7.08–7.01 (m, 2H, CH-3'', CH-5''), 6.75–6.58 (m, 3H, CH-5, CH-7, CH-8), 4.94 (s, 2H, OCH₂Ph-*p*-F), 4.52–4.47 (m, 1H, CH-β), 4.26–4.24 (m, 2H, CH₂-α), 3.57–3.59 (m, 2H, CH₂-3'), 3.23 (s, N(CH₃)₂), 2.95–2.68 (m, 2H, CH₂-4), 2.06–1.53 (m, 6H, CH₂-3, CH₂-1', CH₂-2'), 1.30 (s, 3H, CH₃-2). ¹³C NMR (75 MHz, CDCl₃) δ 162.0 (d, *J* = 244 Hz, C-4''), 152.3 (C-6), 147.6 (C-8a), 139.9 (C-Ph), 129.4 (d, *J*_{CF} = 8 Hz, CH-2'', CH-6''), 128.0 and 127.7 (CH-Ph), 121.7 (C-4a), 117.6 (CH-5), 115.5 (d, *J*_{CF} = 22 Hz, CH-3'', CH-5''), 114.7 and 114.5 (CH-7, CH-8), 74.9 (C-2), 70.0 (OCH₂Ph-*p*-F), 67.7 (CH-β), 65.1 (CH₂-α), 53.0 (N(CH₃)₂), 46.7 (CH₂-3'), 36.0 (CH₂-1'), 31.2 (CH₂-3), 24.8 (CH₂-2'), 23.7 (CH₃-2), 22.0 (CH₂-4). HRMS (ESI) *m/z* calculated for C₃₆H₄₀FNO₂ [M + H]⁺ 538.3116, found: 538.3107.

1-(2-(6-(*p*-Fluorobenzyloxy)-2-methylidihydrobenzopyran-2-yl)ethyl)-6,7-dimethoxy-2,2-dimethyl-1,2,3,4-tetrahydroisoquinolin-2-ium (7c). ¹H NMR (300 MHz, CDCl₃) δ 7.41–7.36 (m, 2H, CH-2'', CH-6''), 7.09–7.03 (m, 2H, CH-3'', CH-5''), 6.73–6.65 (m, 5H, CH-5, CH-7, CH-8, CH-2'', CH-5'''), 4.93 (s, 2H, OCH₂Ph-*p*-F), 4.75–4.70 (m, 1H, CH-3'), 4.02–4.01 (m, 2H, CH₂-α), 3.89 and 3.78 (2 s, 6H,

2*x* OCH₃), 3.50 and 3.30 (2 s, 2*x*NCH₃), 2.82–2.72 (m, 2H, CH₂-4), 2.36–1.40 (m, 8H, CH₂-3, CH₂-1', CH₂-2', CH₂-β), 1.31 (s, CH₃-2). ¹³C NMR (75 MHz, CDCl₃) δ 162 (C-4''), 152.5 (C-6), 148.4 (C-8a), 147.3 (C-3''', C-4'''), 129.4 (d, *J*_{CF} = 8 Hz, CH-2'', CH-6''), 122.0 (C-1'', C-6''), 121.6 (C-4a), 117.7 (CH-5), 115.4 (d, *J*_{CF} = 10 Hz, CH-3'', CH-5''), 115.3 (CH-7), 114.7 (CH-8), 111.0 and 109.0 (CH-2''', CH-5'''), 75.2 (C-2), 70.02 (OCH₂Ph-*p*-F), 66.0 (CH-3'), 56.5 (CH₂-α), 56.2 (OCH₃), 52.0 (NCH₃), 33.8 (CH₂-1'), 31.9 (CH₂-β), 30.9 (CH₂-3), 27.1 (CH₂-2'), 24.7 (CH₃-2), 22.7 (CH₂-4). HRMS (ESI) *m/z* calculated for C₃₂H₃₈FNO₄ [M + H]⁺ 520.2858, found: 520.2844.

General procedure for synthesis of urea benzopyrans 5d, 6d, and 7d. A mixture of 5 (50 mg, 0.11 mmol), 6 (56 mg, 0.11 mmol), 7 (54 mg, 0.11 mmol), 4-chlorophenyl isocyanate (49 mg, 0.32 mmol), and a few drops of Et₃N was dissolved in dry dichloromethane (5 mL) and incubated at room temperature and under N₂ overnight. HCl (15 mL) was added, and the mixture was extracted with dichloromethane (3 × 15 mL) and washed with water and brine. The organic layers were dried over anhydrous Na₂SO₄ and evaporated under reduced pressure. The residue was purified by column chromatography (hexane/EtOAc, 8:2, 9:1, and 6:4 respectively) to yield 46 mg, 67 mg, and 65 mg of compound 5d, 6d, and 7d (68–92% yield), respectively, as colorless oils.

3-(*p*-Chlorophenyl)-*N*-(3-(6-(*p*-fluorobenzyloxy)-2-methylidihydrobenzopyran-2-yl)propyl)-*N*-(*p*-methoxyphenethyl)urea (5d). ¹H NMR (300 MHz, CDCl₃) δ 7.42–7.04 (m, 10H, CH-2'', CH-5'', CH-2''', CH-6''', CH-3''', CH-5''', CH-8''', CH-12''', CH-9''', CH-11'''), 6.89–6.85 (m, 2H, CH-3'', CH-5''), 6.70–6.67 (m, 3H, CH-5, CH-7, CH-8), 4.94 (s, 2H, OCH₂Ph-*p*-F), 3.78 (s, 3H, OCH₃), 3.53–3.48 (m, 2H, CH₂-α), 3.30–3.24 (m, 2H, CH₂-3'), 2.86–2.73 (m, 4H, CH₂-4, CH₂-β), 1.82–1.72 (m, 4H, CH₂-1', CH₂-2'), 1.69–1.60 (m, 2H, CH₂-3), 1.28 (s, CH₃-2). ¹³C NMR (75 MHz, CDCl₃ + 1 drop CD₃OD) δ 162.1 (d, *J*_{CF} = 244 Hz, C-4''), 158.2 (C-4'''), 155.5 (C=O), 152.0 (C-6), 147.6 (C-8a), 137.5 (C-7'''), 132.9 (d, *J* = 3 Hz, C-1''), 130.9 (C-10'''), 129.7 (C-1'''), 129.2 (d, *J*_{CF} = 8 Hz, CH-2'', CH-6''), 128.6 (CH-2''', CH-6'''), 121.7 (C-4a), 121.3 (CH-9''', CH-11'''), 120.0 (CH-8''', CH-12'''), 117.4 (CH-5), 115.2 (CH-7), 115.2 (d, *J*_{CF} = 21 Hz, CH-3'', CH-5''), 114.4 (CH-8), 114.1 (CH-3''', CH-5'''), 75.8 (C-2), 69.9 (OCH₂Ph-*p*-F), 55.1 (OCH₃), 49.7 (CH₂-α), 47.7 (CH₂-3'), 36.0 (CH₂-1'), 33.8 (CH₂-β), 31.0 (CH₂-3), 23.6 (CH₃-2), 22.2 (CH₂-2'), 22.1 (CH₂-4). HRMS (ESI) *m/z* calculated for C₃₆H₃₈ClFN₂O₄ [M]⁺ 617.2575, found: 617.2576.

3-(*p*-Chlorophenyl)-*N*-(2,2-diphenylethyl)-*N*-(3-(6-(*p*-fluorobenzyloxy)-2-methylidihydrobenzopyran-2-yl)propyl)urea (6d). ¹H NMR (300 MHz, CDCl₃) δ 7.46 (d, *J* = 8.8 Hz, 2H, CH-2'', CH-6''), 7.43–6.97 (m, 16H, 2*x* Ph, CH-8''', CH-11''', CH-9''', CH-12''', CH-3'', CH-5''), 6.71–6.21 (m, 3H, CH-5, CH-7, CH-8), 4.93 (s, 2H, OCH₂Ph-*p*-F), 4.35 (t, *J* = 7.4 Hz, 1H, CH-β), 3.95 (d, *J* = 7.4 Hz, 2H, CH₂-α), 3.19–3.12 (m, 2H, CH₂-3'), 2.76–2.70 (m, 2H, CH₂-4), 1.80–1.70 (m, 2H, CH₂-3), 1.55–1.50 (m, 4H, CH₂-1', CH₂-2'), 1.25 (s, 3H, CH₃-2). ¹³C NMR (75 MHz, CDCl₃) δ 162.0 (d, *J*_{CF} = 244 Hz, C-4''), 155.4 (C=O), 152.2 (C-6), 147.8 (C-8a), 142.0 (d, *J* = 2

Hz, C-Ph), 137.8 (C-1^m), 133.1 (d, J_{CF} = 3 Hz, C-1ⁿ), 129.8 (C-4^m), 129.4 (d, J_{CF} = 8 Hz, CH-2ⁿ, CH-6ⁿ), 128.6 and 127.5 (CH-Ph), 127.1 (CH-9^m, CH-11^m), 121.7 (C-4a), 121.0 (CH-8^m, CH-12^m), 117.7 (CH-5), 115.6 (d, J_{CF} = 19 Hz, CH-3ⁿ, CH-5ⁿ), 115.3 (CH-7), 114.5 (CH-8), 75.9 (C-2), 70.0 (OCH₂Ph-*p*-F), 53.8 (CH₂-α), 49.9 (CH-β), 48.2 (CH₂-3ⁿ), 36.3 (CH₂-1ⁿ), 31.2 (CH₂-3), 24.0 (CH₃-2), 22.4 (CH₂-2ⁿ), 22.1 (CH₂-4). HRMS (ESI) m/z calculated for C₄₁H₄₀ClFN₂O₃ [M]⁺ 663.2784, found: 663.2764.

***N*-(*p*-Chlorophenyl)-1-(2-(6-(*p*-fluorobenzyl)oxy)-2-methyl-dihydrobenzopyran-2-yl)ethyl)-6,7-dimethoxy-3,4-dihydroisoquinoline-2(1H)-carboxamide (7d).** ¹H NMR (300 MHz, CDCl₃ + 1 drop CD₃OD) δ 7.37–7.1 (m, 6H, CH-2ⁿ, CH-6ⁿ, CH-8^m, CH-12^m, CH-9^m, CH-11^m), 7.08–6.89 (m, 2H, CH-3ⁿ, CH-5ⁿ), 6.68–6.58 (m, 5H, CH-5, CH-7, CH-8, CH-2^m, CH-5^m), 4.87 (s, 2H, OCH₂Ph-*p*-F), 4.08–4.03 (m, 1H, CH-3ⁿ), 3.79 and 3.77 (2s, 6H, 2xOCH₃), 3.19 and 2.91 (2m, 2H, CH₂-α), 2.74–2.67 (m, 4H, CH₂-4, CH₂-β), 1.93–1.65 (m, 6H, CH₂-3, CH₂-1ⁿ, CH₂-2ⁿ), 1.31 (s, 3H, CH₃-2). ¹³C NMR (75 MHz, CDCl₃ + 1 drop CD₃OD) δ 162.1 (C-4ⁿ), 155.2 (C=O), 152.3 (C-6), 148.1 (C-8a), 147.5 (C-3^m, C-4^m), 138.0 (C-7^m), 133.2 (C-1ⁿ), 131.2 (C-10^m), 131.0 (CH-2ⁿ, CH-6ⁿ), 127.1 (C-1^m, C-6^m), 121.6 (CH-9^m, CH-11^m), 120.3 (CH-8^m, CH-12^m), 117.7 (CH-5), 115.5 (CH-3ⁿ, CH-5ⁿ), 115.2 (CH-7), 114.4 (CH-8), 111.9 and 109.2 (CH-2^m, CH-5^m), 75.6 (C-2), 70.0 (OCH₂Ph-*p*-F), 57.0 (CH-3ⁿ), 55.8 and 55.7 (OCH₃), 32.1 (CH₂-1ⁿ), 31.4 (CH₂-3), 30.4 (CH₂-2ⁿ), 28.1 (CH₂-α), 24.0 (CH₃-2), 23.1 (CH₂-4, CH₂-β). HRMS (ESI) m/z calculated for C₃₇H₃₈ClFN₂O₂ [M]⁺ 645.2526, found: 645.2512.

4.2. Pharmacology

Cell culture. Human TNBC (MDA-MB-231 and MDA-MB-436) and normal breast epithelial (MCF10A) cell lines were obtained from the American Type Culture Collection (ATCC) (LGC Standards, S.L.U. Barcelona, Spain) and cultured in a humidified air incubator at 37 °C and 5% CO₂. Cells were grown in Dulbecco's modified Eagle's medium (DMEM) with nutrient mixture Ham's F-12 (DMEM/F12) supplemented with 10% (v/v) fetal bovine serum (FBS), 2% penicillin/streptomycin, and 1% glutamine.

Cell viability. The cytotoxic effects of the different compounds in the TNBC cells were determined using a water-soluble tetrazolium dye (WST-1) assay kit (K304-2500, Deltaclon, Madrid, Spain). Cells were seeded at 6×10^3 cells per well in 96-well plates. After 24 hours, the cells were treated with different doses of compounds (2.5 μM to 100 μM) or DMSO for negative control groups (0.1%). WST-1 solution at 7% in DMEM-F12 without phenol red was added for 3 hours. The absorbance was then measured at 450 nm and background corrected at 650 nm using Spectra Max Plus (Thermo Fisher Scientific, Waltham, MA, USA). The percentage of viable cells was calculated by setting the negative control group cells to 100%.

Apoptosis/necrosis assay. Apoptosis/necrosis cell death was studied using an Annexin V-FITC/PI dual staining assay. MDA-MB-231 and MDA-MB-436 cells (3×10^4 cells per well) were seeded in 24-well plates and allowed to grow overnight.

The medium was then replaced with the different compounds at their IC₅₀ values or DMSO for negative control groups (0.1%) in complete medium. Then, all cells were processed with the Annexin V-assay kit (ANXCKF7, Immunostep, Salamanca, Spain) according to the manufacturer's instructions. A Becton Dickinson LSR Fortessa cytometer (BD Biosciences, Franklin Lakes, NJ, USA) was used for samples, and cell analyses were performed using BD FACSDiva X20 software.

ROS measurement. MDA-MB-231 and MDA-MB-436 cells were seeded at 2.5×10^4 cells per well in 8-well slides. The following day, the cells were treated with compounds at their IC₂₅ values, DMSO for negative control groups (0.05%), or TBHP at 100 μM for 48 hours. The medium was then replaced with DCFDA at 10 μM (ab113851 DCFDA/H2DCFDA – Cellular ROS Assay Kit, Abcam, Cambridge, UK) in complete medium, and the cells were then incubated for 45 minutes at room temperature in the dark. The fluorescence intensity from each sample was captured by LEICA DMi8 fluorescence microscopy, and images analysis was performed using ImageJ software.

Cell cycle. Cell cycle analysis was carried out to estimate the distribution of the cell population in the different phases of the cell cycle. First, 1.5×10^5 cells per well were seeded in 6-well plates and allowed to grow overnight. The medium was then replaced with the different compounds at their IC₅₀ values or DMSO for negative control groups (0.1%) in complete medium. After 48 hours, untreated and treated cells were harvested, washed with phosphate-buffered saline (PBS), and fixed in ice-cold 70% ethanol for at least 1 hour at –20 °C. Cells were then stained with PI/RNASE solution (PI/RNASE, Immunostep, Salamanca, Spain) and incubated for 24 hours at 4 °C. A BD LSR Fortessa cytometer (BD Biosciences, Franklin Lakes, NJ, USA) was used for samples, and cell analyses were performed using ModFit 4.1 software.

Determination of mRNA expression by quantitative RT-PCR. TNBC cells (1×10^6 cells per well) were seeded in 6-well plates and allowed to grow overnight. The medium was then replaced with the different compounds at their IC₂₅ values or DMSO for negative control groups (0.05%) in complete medium. Total RNA was extracted from mice WAT and liver samples by homogenization using TRIzol RNA Isolation Reagent (Life Technologies, Thermo Fisher Scientific, Waltham, MA) and purified by standard methods. Reverse transcription was performed on 1000 ng of total RNA with a high-capacity cDNA reverse transcription kit (Applied Biosystems, Thermo Fisher Scientific, Waltham, MA). Relative quantification of *Bcl-2*, *CCND1*, and *CCNE2* was determined with the 2^{–ΔΔCt} method using *Gapdh* (Applied Biosystems) as an endogenous control and normalized to the vehicle group.

Statistical analysis. The data are presented as the mean ± SD or ± SEM. Statistical analyses were carried out by one-way or two-way ANOVA, followed by Tukey's or Dunnett's multiple comparisons test (GraphPad Prism 9). Differences with a *p*-value < 0.05 were considered statistically different.

Conflicts of interest

The authors declare that they have no known competing financial interests or personal relationships that could have appeared to influence the work reported in this paper.

Acknowledgements

This work was supported by the Carlos III Health Institute (ISCIII) and the European Regional Development Fund (FEDER) by grant numbers PI21/02045 and PI21/01351, and the Generalitat Valenciana (GVA) by grant numbers AICO/2021/081 and APOTIP/2020/011. Nuria Cabedo was funded by the ISCIII Miguel Servet programme (CPII20/00010), co-funded by the European Social Fund. Carlos Villarroel-Vicente was funded by the ISCIII (PFIS – FI19/00153), Ainhoa García by the GVA (AICO/2021/081), and Sandra Torres-Ruiz by a pre-doctoral grant (ACIF/2019/119).

References

- 1 H. Şenol, P. Tulay, M. Ç. Ergören, A. Hanoğlu, İ. Çalış and G. Mocan, Cytotoxic effects of verbascoside on MCF-7 and MDA-MB-231, *Turk. J. Pharm. Sci.*, 2020, **18**, 637–644, DOI: [10.4274/tjps.galenos.2021.36599](https://doi.org/10.4274/tjps.galenos.2021.36599).
- 2 K. R. Senwar, T. S. Reddy, D. Thummuri, P. Sharma, V. G. Naidu, G. Srinivasulu and N. Shankaraiah, Design, synthesis and apoptosis inducing effect of novel (Z)-3-(3'-methoxy-4'-(2-amino-2-oxoethoxy)-benzylidene)indolin-2-ones as potential antitumor agents, *Eur. J. Med. Chem.*, 2026, **118**, 34–36, DOI: [10.1016/j.ejmech.2016.04.025](https://doi.org/10.1016/j.ejmech.2016.04.025).
- 3 R. L. Siegel, K. D. Miller and A. Jemal, Cancer statistics, 2015, *Ca-Cancer J. Clin.*, 2015, **65**, 5–29, DOI: [10.3322/caac.21254](https://doi.org/10.3322/caac.21254).
- 4 I. Ahmad and W. Shagufta, Recent developments in steroidal and nonsteroidal aromatase inhibitors for the chemoprevention of estrogen-dependent breast cancer, *Eur. J. Med. Chem.*, 2015, **102**, 375–386, DOI: [10.1016/j.ejmech.2015.08.010](https://doi.org/10.1016/j.ejmech.2015.08.010).
- 5 A. G. Waks and E. P. Winer, Breast cancer treatment: a review, *JAMA, J. Am. Med. Assoc.*, 2019, **321**, 288–300, DOI: [10.1001/jama.2018.19323](https://doi.org/10.1001/jama.2018.19323).
- 6 O. A. Bamodu, W. C. Huang, D. T. Tzeng, A. Wu, L. S. Wang, C. T. Yeh and T. Y. Chao, Ovatodiolide sensitizes aggressive breast cancer cells to doxorubicin, eliminates their cancer stem cell-like phenotype, and reduces doxorubicin-associated toxicity, *Cancer Lett.*, 2015, **364**, 125–134, DOI: [10.1016/j.canlet.2015.05.006](https://doi.org/10.1016/j.canlet.2015.05.006).
- 7 M. Gallorini, A. Cataldi and A. di Giacomo, Cyclin-dependent kinase modulators and cancer therapy, *BioDrugs*, 2012, **26**, 377–391, DOI: [10.1007/BF03261895](https://doi.org/10.1007/BF03261895).
- 8 D. Nandini, A. Jennifer and D. Pradip, Therapeutic strategies for metastatic triple-negative breast cancers: from negative to positive, *Pharmaceuticals*, 2021, **14**, 455–472, DOI: [10.3390/ph14050455](https://doi.org/10.3390/ph14050455).
- 9 M. Brown, A. Tsodikov, K. R. Bauer, C. A. Parise and V. Caggiano, The role of human epidermal growth factor receptor 2 in the survival of women with estrogen and progesterone receptor-negative, invasive breast cancer, The California Cancer Registry, 1999–2004, *Cancer*, 2008, **112**, 737–747, DOI: [10.1002/cncr.23243](https://doi.org/10.1002/cncr.23243).
- 10 M. Liao, J. Zhang, G. Wang, L. Wang, J. Liu, L. Ouyang and B. Liu, Small-molecule drug discovery in triple negative breast cancer: current situation and future directions, *J. Med. Chem.*, 2021, **64**, 2382–2418, DOI: [10.1021/acs.jmedchem.0c01180](https://doi.org/10.1021/acs.jmedchem.0c01180).
- 11 O. Gluz, C. Liedtke, N. Gottschalk, L. Pusztail, U. Nitz and N. Harbeck, Triple-negative breast cancer – current status and future directions, *Ann. Oncol.*, 2009, **20**, 1913–1927, DOI: [10.1093/annonc/mdp492](https://doi.org/10.1093/annonc/mdp492).
- 12 Y. Li, S. Li, X. Meng, R. Y. Gan, J. J. Zhang and H. B. Li, Dietary natural products for prevention and treatment of breast cancer, *Nutrients*, 2017, **9**, 728, DOI: [10.3390/nu9070728](https://doi.org/10.3390/nu9070728).
- 13 Q. Zhao, M. Zhao, A. B. Parris, Y. Xing and X. Yang, Genistein targets the cancerous inhibitor of PP2A to induce growth inhibition and apoptosis in breast cancer cells, *Int. J. Oncol.*, 2016, **49**, 1203–1210, DOI: [10.3892/ijo.2016.3588](https://doi.org/10.3892/ijo.2016.3588).
- 14 J. Chen, Y. Duan, X. Zhang, Y. Ye, B. Ge and J. Chen, Genistein induces apoptosis by the inactivation of the IGF-1R/p-Akt signaling pathway in MCF-7 human breast cancer cells, *Food Funct.*, 2015, **6**, 995–1000, DOI: [10.1039/c4fo01141d](https://doi.org/10.1039/c4fo01141d).
- 15 S. S. Bhat, S. K. Prasad, C. Shivamallu, K. S. Prasad, A. Syed, P. Reddy, C. A. Cull and R. G. Amachawadi, Genistein: a potent anti-breast cancer agent, *Curr. Issues Mol. Biol.*, 2021, **43**, 1502–1517, DOI: [10.3390/cimb43030106](https://doi.org/10.3390/cimb43030106).
- 16 Y. Safdari, M. Khalili, M. A. Ebrahimzadeh, Y. Yazdani and S. Farajnia, Natural inhibitors of PI3K/AKT signaling in breast cancer: emphasis on newly-discovered molecular mechanisms of action, *Pharmacol. Res.*, 2015, **93**, 1–10, DOI: [10.1016/j.phrs.2014.12.004](https://doi.org/10.1016/j.phrs.2014.12.004).
- 17 A. A. Abd El-Hafeez, H. O. Khalifa, E. A. M. Mahdy, V. Sharma, T. Hosoi, P. Ghosh, K. Ozawa, M. M. Montano, T. Fujimura, A. R. N. Ibrahim, M. A. A. Abdelhamid, S. P. Pack, S. A. Shouman and S. Kawamoto, Anticancer effect of norwogonin (5, 7, 8-trihydroxyflavone) on human triple-negative breast cancer cells via downregulation of TAK1, NF-κB, and STAT3, *Pharmacol. Rep.*, 2019, **71**, 289–298, DOI: [10.1016/j.pharep.2019.01.001](https://doi.org/10.1016/j.pharep.2019.01.001).
- 18 S. Sordon, J. Popłoński, M. Milczarek, M. Stachowicz, T. Tronina, A. Z. Kucharska, J. Wietrzyk and E. Huszcza, Structure-antioxidant-antiproliferative activity relationships of natural C7 and C7-C8 hydroxylated flavones and flavanones, *Antioxidants*, 2019, **8**, 210, DOI: [10.3390/antiox8070210](https://doi.org/10.3390/antiox8070210).
- 19 K. M. Yap, M. Sekar, Y. S. Wu, S. H. Gan, N. N. I. M. Rani, L. J. Seow, V. Subramaniam, N. K. Fuloria, S. Fuloria and P. T. Lum, Hesperidin and its aglycone hesperetin in breast cancer therapy: A review of recent developments and future prospects, *Saudi J. Biol. Sci.*, 2021, **28**, 6730–6747, DOI: [10.1016/j.sjbs.2021.07.046](https://doi.org/10.1016/j.sjbs.2021.07.046).
- 20 S. Rani, K. Raheja, V. Luxami and K. Paul, A review on diverse heterocyclic compounds as the privileged scaffolds in non-steroidal aromatase inhibitors, *Bioorg. Chem.*, 2021, **113**, 105017, DOI: [10.1016/j.bioorg.2021.105017](https://doi.org/10.1016/j.bioorg.2021.105017).
- 21 C. Zhang, Z. Wang, Y. Shi, B. Yu and Y. Song, Recent advances of LSD1/KDM1A inhibitors for disease therapy, *Bioorg. Chem.*, 2023, **134**, 106443, DOI: [10.1016/j.bioorg.2023.106443](https://doi.org/10.1016/j.bioorg.2023.106443).

- 22 M. C. Gonzalez, A. Serrano, M. C. Zafra-Polo, D. Cortes and K. S. Rao, Polycerasoidin and polycerasoidol, two new prenylated benzopyran derivatives from *Polyalthia cerasoides*, *J. Nat. Prod.*, 1995, **58**, 1278–1284, DOI: [10.1021/np50122a022](https://doi.org/10.1021/np50122a022).
- 23 M. C. Zafra-Polo, M. C. González, J. R. Tormo, E. Estornell and D. Cortes, Polyalthidin: new prenylated benzopyran inhibitor of the mammalian mitochondrial respiratory chain, *J. Nat. Prod.*, 1996, **59**, 913–916, DOI: [10.1021/np960492m](https://doi.org/10.1021/np960492m).
- 24 A. Bermejo, A. Collado, I. Barrachina, P. Marqués, N. El Aouad, X. Franck, F. Garibotto, C. Dacquet, D. H. Caignard, F. D. Suvire, R. D. Enriz, L. Piqueras, B. Figadère, M. J. Sanz, N. Cabedo and D. Cortes, Polycerasoidol, a natural prenylated benzopyran with a dual PPAR α /PPAR γ agonist activity and anti-inflammatory effect, *J. Nat. Prod.*, 2019, **82**, 1802–1812, DOI: [10.1021/acs.jnatprod.9b00003](https://doi.org/10.1021/acs.jnatprod.9b00003).
- 25 P. Marques, C. Villarroya-Vicente, A. Collado, A. García, L. Vila, I. Duplan, N. Hennuyer, F. Garibotto, R. D. Enriz, C. Dacquet, B. Staels, L. Piqueras, D. Cortes, M. J. Sanz and N. Cabedo, Anti-inflammatory effects and improved metabolic derangements in ob/ob mice by a newly synthesized prenylated benzopyran with pan-PPAR activity, *Pharmacol. Res.*, 2023, **187**, 106638, DOI: [10.1016/j.phrs.2022.106638](https://doi.org/10.1016/j.phrs.2022.106638).
- 26 H. Taha, C. Y. Looi, A. Arya, W. F. Wong, L. F. Yap, M. Hasanpourghadi, M. A. Mohd, I. C. Paterson and H. Mohd Ali, (6E,10E) Isopolycerasoidol and (6E,10E) isopolycerasoidol methyl ester, prenylated benzopyran derivatives from *pseuduvaria monticola* induce mitochondrial-mediated apoptosis in human breast adenocarcinoma cells, *PLoS One*, 2015, **10**, e0126126, DOI: [10.1371/journal.pone.0126126](https://doi.org/10.1371/journal.pone.0126126).
- 27 B. C. Pearce, R. A. Parker, M. E. Deason, D. D. Dischino, E. Gillespie, A. A. Qureshi, K. Volk and J. J. Wright, Inhibitors of cholesterol biosynthesis. 2. Hypocholesterolemic and antioxidant activities of benzopyran and tetrahydronaphthalene analogues of the tocotrienols, *J. Med. Chem.*, 1994, **37**, 526–541, DOI: [10.1021/jm00030a012](https://doi.org/10.1021/jm00030a012).
- 28 A. Bermejo, I. Barrachina, N. El Aouad, X. Franck, N. Chahboune, I. Andreu, B. Figadère, L. Vila, N. Hennuyer, B. Staels, C. Dacquet, D. H. Caignard, M. J. Sanz, D. Cortes and N. Cabedo, Synthesis of benzopyran derivatives as PPAR α and/or PPAR γ activators, *Bioorg. Med. Chem.*, 2019, **27**, 115162, DOI: [10.1016/j.bmc.2019.115162](https://doi.org/10.1016/j.bmc.2019.115162).
- 29 A. García, L. Vila, P. Marín, Á Bernabeu, C. Villarroya-Vicente, N. Hennuyer, B. Staels, X. Franck, B. Figadère, N. Cabedo and D. Cortes, Synthesis of 2-prenylated alkoxyated benzopyrans by horner-wadsworth-emmons olefination with PPAR α/γ agonist activity, *ACS Med. Chem. Lett.*, 2021, **12**, 1783–1786, DOI: [10.1021/acsmedchemlett.1c00400](https://doi.org/10.1021/acsmedchemlett.1c00400).
- 30 L. Vila, N. Cabedo, C. Villarroya-Vicente, A. García, Á Bernabeu, N. Hennuyer, B. Staels, X. Franck, B. Figadère, M. J. Sanz and D. Cortes, Synthesis and biological studies of “Polycerasoidol” and “trans- δ -Tocotrienolic acid” derivatives as PPAR α and/or PPAR γ agonists, *Bioorg. Med. Chem.*, 2022, **53**, 116532, DOI: [10.1016/j.bmc.2021.116532](https://doi.org/10.1016/j.bmc.2021.116532).
- 31 A. K. Ghosh and M. Brindisi, Urea derivatives in modern drug discovery and medicinal chemistry, *J. Med. Chem.*, 2020, **63**, 2751–2788, DOI: [10.1021/acs.jmedchem.9b01541](https://doi.org/10.1021/acs.jmedchem.9b01541).
- 32 M. Redza-Dutordoir and D. A. Averill-Bates, Activation of apoptosis signalling pathways by reactive oxygen species, *Biochim. Biophys. Acta*, 2016, **1863**, 2977–2992, DOI: [10.1016/j.bbamer.2016.09.012](https://doi.org/10.1016/j.bbamer.2016.09.012).
- 33 J. M. Adams and S. Cory, The BCL-2 arbiters of apoptosis and their growing role as cancer targets, *Cell Death Differ.*, 2018, **25**, 27–36, DOI: [10.1038/cdd.2017.161](https://doi.org/10.1038/cdd.2017.161).
- 34 J. C. Martinou and R. J. Youle, Mitochondria in apoptosis: Bcl-2 family members and mitochondrial dynamics, *Dev. Cell*, 2011, **21**, 92–101, DOI: [10.1016/j.devcel.2011.06.017](https://doi.org/10.1016/j.devcel.2011.06.017).
- 35 S. Cory and J. M. Adams, The Bcl2 family: Regulators of the cellular life-or-death switch, *Nat. Rev. Cancer*, 2002, **2**, 647–656, DOI: [10.1038/nrc883](https://doi.org/10.1038/nrc883).
- 36 H. Guo, H. Cui, X. Peng, J. Fang, Z. Zuo, J. Deng, X. Wang, B. Wu, K. Chen and J. Deng, Modulation of the PI3K/Akt Pathway and Bcl-2 Family Proteins Involved in Chicken's Tubular Apoptosis Induced by Nickel Chloride (NiCl₂), *Int. J. Mol. Sci.*, 2015, **16**, 22989–23011, DOI: [10.3390/ijms160922989](https://doi.org/10.3390/ijms160922989).
- 37 I. Neganova and M. Lako, G1 to S phase cell cycle transition in somatic and embryonic stem cells, *J. Anat.*, 2008, **213**, 30–44, DOI: [10.1111/j.1469-7580.2008.00931.x](https://doi.org/10.1111/j.1469-7580.2008.00931.x).
- 38 B. Stecca and E. Rovida, Impact of ERK5 on the Hallmarks of Cancer, *Int. J. Mol. Sci.*, 2019, **20**, 1426, DOI: [10.3390/ijms20061426](https://doi.org/10.3390/ijms20061426).
- 39 R. Paudel, L. Fusi and M. Schmidt, The MEK5/ERK5 Pathway in Health and Disease, *Int. J. Mol. Sci.*, 2021, **22**, 7594, DOI: [10.3390/ijms22147594](https://doi.org/10.3390/ijms22147594).
- 40 W. Song, L. Tang, Y. Xu, J. Xu, W. Zhang, H. Xie, S. Wang and X. Guan, PARP inhibitor increases chemosensitivity by upregulating miR-664b-5p in BRCA1-mutated triple-negative breast cancer, *Sci. Rep.*, 2017, **7**, 42319, DOI: [10.1038/srep42319](https://doi.org/10.1038/srep42319).
- 41 W. Song, L. Tang, Y. Xu, J. Xu, W. Zhang, H. Xie, S. Wang and X. Guan, PARP inhibitor increases chemosensitivity by upregulating miR-664b-5p in BRCA1-mutated triple-negative breast cancer, *Sci. Rep.*, 2017, **7**, 42319, DOI: [10.1038/srep42319](https://doi.org/10.1038/srep42319).